Journal of Geophysical Research: Planets

RESEARCH ARTICLE
10.1029/2017JE005493

Key Points:
- Rover data indicate that phosphorous was essentially immobile at all stages in the formation of the sulfate-rich bedrocks at Meridiani
- Results from a terrestrial analog and lab experiments confirm that P can be immobile under some acid-sulfate conditions
- Potential reservoirs for P include basaltic glass, Fe- or Al-phosphates, alunite-jarosite group minerals, and surface adsorption

Supporting Information:
- Supporting Information S1
- Data Set S1
- Data Set S2
- Data Set S3

Correspondence to:
T. M. McCollom,
mccollom@lasp.colorado.edu

Citation:
McCollom, T. M., Donaldson, C., Moskowitz, B., Berquó, T. S., & Hynek, B. (2018). Phosphorous immobility during formation of the layered sulfate deposits of the Burns formation at Meridiani Planum. *Journal of Geophysical Research: Planets*, *123*, 1230–1254. https://doi.org/10.1029/2017JE005493

Received 17 NOV 2017
Accepted 30 APR 2018
Accepted article online 6 MAY 2018
Published online 23 MAY 2018

Phosphorous Immobility During Formation of the Layered Sulfate Deposits of the Burns Formation at Meridiani Planum

Thomas M. McCollom[1], Chris Donaldson[1], Bruce Moskowitz[2,3], Thelma S. Berquó[4], and Brian Hynek[1,5]

[1]Laboratory for Atmospheric and Space Physics, University of Colorado Boulder, Boulder, CO, USA, [2]Department of Earth Sciences, University of Minnesota, Minneapolis, MN, USA, [3]Institute for Rock Magnetism, University of Minnesota, Minneapolis, MN, USA, [4]Department of Physics, Concordia College, Moorhead, MN, USA, [5]Department of Geological Sciences, University of Colorado Boulder, Boulder, CO, USA

Abstract The relatively high abundance of phosphorous (P) in rocks from the Martian crust makes it a potentially useful element for tracking geochemical processes. Owing to the high solubility of common P-bearing minerals such as apatite at low pH, P is widely thought to be mobile under acid-sulfate conditions. Accordingly, transport of P by acidic fluids has been invoked to explain enrichments or depletions of this element in some rocks and soils from Mars. The sediments that compose the layered-sulfate deposits of the Burns formation at Meridiani Planum were originally derived from a basaltic precursor but appear to have been exposed to acidic, sulfate-rich fluids at several intervals during their history. Yet, assessment of the chemical composition of the bedrocks indicates that they maintain pristine igneous P:Ti ratios and P abundances similar to Martian basalts, indicating that there has been little or no transport of P into or out of the deposits at any stage in their formation. Potential reservoirs for P in the deposits include basaltic glass, secondary Fe- or Al-phosphate minerals, substitution of PO_4 for SO_4 in alunite-jarosite group minerals, or surface adsorption. Although Fe-phosphates were not among the minerals detected by the Mössbauer spectrometer onboard the Opportunity rover at Meridiani, it might be difficult to detect such minerals even if they are present because they are below the detection limit or have signatures similar to other minerals. Overall, the results demonstrate that P can be immobile even in some acid-sulfate environments on Mars and Earth.

Plain Language Summary The bedrocks at the landing site of the Opportunity rover on Meridiani Panum, Mars, are standstones composed of sulfate mineral and altered basalt components. The sand was deposited at Meridiani by wind and water, and then underwent further mineral and chemical alteration by infiltrating groundwater. At several stages during formation of the bedrocks, the sediments interacted with acidic, sulfate-rich fluids. The element phosphorous is commonly thought to be mobile under acidic conditions, and transport by acidic fluids is thought to be responsible for addition or removal of phosphorous in some rocks and soils at other locations on Mars. Yet analysis of chemical data obtained by the Opportunity rover at Meridiani indicates that phosphorous was not transported into or out of the rocks to any significant degree, despite the influx of acidic fluids at several intervals during their formation. This result provides a new constraint that can be used to test alternative models for the origin of the bedrocks.

1. Introduction

Rocks from the surface of Mars contain sufficient amounts of phosphorous to be quantified in situ by instruments such as the Alpha Particle X-ray Spectrometers (APXS) that have been deployed on several rovers (Gellert et al., 2006; Rieder et al., 2004; Wänke et al., 2001). Results from these instruments, as well as analyses of Martian meteorites (McSween & Treiman, 1998), indicate that basaltic rocks from the Martian surface are, in general, substantially enriched in P compared to their terrestrial counterparts. For instance, basaltic rocks from Gusev crater analyzed by the Spirit rover contain up to 5.2 wt% P_2O_5, with most samples having abundances between 0.6 and 1.4 wt% (Gellert et al., 2006; Ming et al., 2006, 2008). For comparison, terrestrial mid-ocean ridge basalts typically contain ~0.14 wt% P_2O_5, while ocean-island basalts contain ~0.6 wt% P_2O_5 on average (Sun & McDonough, 1989).

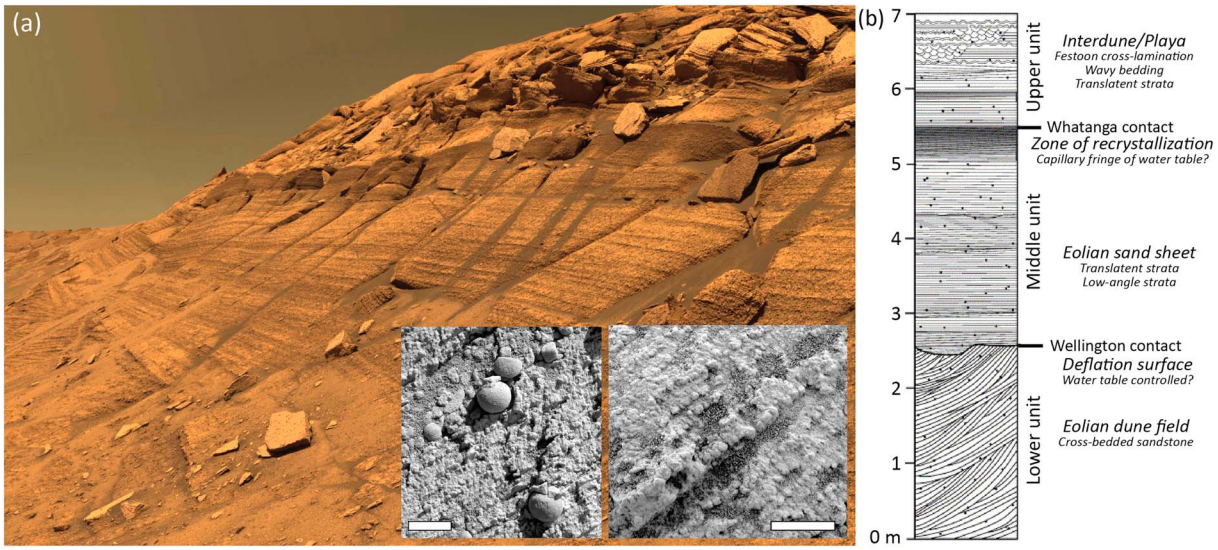

Figure 1. Overview of the Burns formation at Meridiani Planum, Mars. (a) Cross section of Burns formation exposed at Burns cliff on the southeast rim of Endurance crater. Insets are close-up views of the deposits showing the presence of 0.1–1.0 mm sand grains and fine-scale laminations. Note the presence of spheroidal hematite "blueberries" in the left image. Scale bars are approximately 5 mm. Close-up images were obtained on sol 142 (left) and sol 41 (right). (b) Stratigraphy of the Burns formation, adapted from Grotzinger et al. (2005).

The predominant igneous phosphate minerals in Martian meteorites are Cl-rich apatite [$Ca_5(PO_4)_3(Cl,OH,F)$] and merrillite [$Ca_9NaMg(PO_4)_7$] (e.g., McSween & Treiman, 1998). These are likely to be the predominant mineral reservoirs for P in basaltic rocks exposed at the surface as well (e.g., Adcock & Hausrath, 2015; McSween et al., 2008). Apatite and merrillite have relatively high aqueous solubilities and dissolve rapidly under acidic conditions (e.g., Adcock et al., 2013; Guidry & Mackenzie, 2003; Harouiya et al., 2007). As a consequence, P has the potential to serve as a tracer of acidic alteration on Mars, and mobilization of P during interaction with acidic aqueous solutions has been invoked to explain enrichments and depletions of this element in some Martian rocks and soils (Adcock & Hausrath, 2015; Gellert et al., 2006; Greenwood & Blake, 2006; Hausrath et al., 2013; Hurowitz et al., 2006; Ming et al., 2006, 2008; Rieder et al., 2004; Yen et al., 2008).

The layered sulfate-rich deposits that comprise the Burns formation at Meridiani Planum (Figure 1) also contain relatively high P contents, with average measured P_2O_5 concentrations of 1.05 wt% (Arvidson et al., 2015; Rieder et al., 2004). Proposed models for formation of the deposits invoke interaction of silicate materials derived from a basaltic source with acidic, sulfate-rich fluids, and most likely involved multiple episodes of fluid-rock interaction (Berger et al., 2009; Hurowitz & Fischer, 2014; McLennan et al., 2005; McCollom & Hynek, 2005; Niles & Michalski, 2009; Squyres et al., 2004; Squyres, Knoll, et al., 2006; Tréguier et al., 2008; Zolotov & Shock, 2005). To date, however, the possibility that P may have been mobilized into or out of the deposits during these interactions with acid-sulfate fluids has not been thoroughly evaluated.

In this study, the geochemistry of the Burns formation bedrocks was assessed for evidence of mobilization of P. Mobility of this element was assessed by comparison of the P abundance and P:Ti ratios in the Burns formation deposits with those measured in Martian basalts by the Pathfinder, Spirit, and Opportunity rovers, as well as with basaltic Martian meteorites. Additional insights are provided by studies of the behavior of P during acid-sulfate alteration of basalt in a terrestrial fumarolic setting and during laboratory simulation of basalt alteration. The results provide additional constraints on element mobility during development of the layered deposits and proposed scenarios for their formation.

2. Geologic Overview of the Burns Formation

The layered bedrocks that comprise the Burns formation have been described as impure sandstones, composed of a mixture of sulfate and silicate mineral components (Clark et al., 2005; Glotch & Bandfield, 2006; Grotzinger et al., 2005; McLennan et al., 2005). Textural and geochemical evidence indicates that the framework of the sandstones is composed of sulfate-cemented siliciclastic sand grains (Figure 1; Grotzinger et al., 2005; McLennan et al., 2005; Squyres, Knoll, et al., 2006). Distinct cross-bedding and other morphological

features indicate that the sulfate-cemented sand particles were transported and deposited at their current location by eolian and fluvial processes (Figure 1; Grotzinger et al., 2005). Subsequent infiltration of the deposits by one or more generations of groundwater led to diagenetic alteration of the sediments that included dissolution of some minerals and precipitation of pore-filling cements, along with formation of the distinctive hematite spherules that are characteristic of the site (McLennan et al., 2005).

Geochemical analysis of Burns formation bedrocks by the APXS onboard the Opportunity rover indicates that their composition closely resembles that of Martian basalt except for the addition of a sulfur component, most likely in the form of sulfate, and extensive oxidation of Fe (e.g., McCollom & Hynek, 2005; Squyres et al., 2004; Squyres, Arvidson, et al., 2006). For this reason, scenarios for the formation of the deposits focus on addition of an oxidized sulfur component to siliciclastic materials derived from a basaltic provenance (Berger et al., 2009; McLennan et al., 2005; McCollom & Hynek, 2005; Niles & Michalski, 2009; Squyres et al., 2004; Squyres, Knoll, et al., 2006; Tréguier et al., 2008). Since the framework of the bedrocks appears to consist of sulfate-cemented siliciclastic grains, the addition of the sulfur component evidently took place prior to the deposition of the materials at their present location (Grotzinger et al., 2005; McLennan et al., 2005; Squyres, Knoll, et al., 2006).

The Opportunity rover was not equipped with instrumentation to directly determine the mineralogy of the bedrocks. However, their mineral composition can be modeled based on other observations. Estimates of the mineral composition vary somewhat depending on assumptions, but models indicate the rocks are composed of ~30–40% siliciclastic materials (including plagioclase, pyroxenes, and nontronite or other phyllosilicates), 15–25% amorphous silica and/or glass, 5–10% hematite and other Fe-oxides/oxyhydroxides, and ~30–40% Mg-, Fe-, and Ca-sulfate minerals including natrojarosite, along with minor chloride and phosphate components (Clark et al., 2005; Glotch et al., 2006; Glotch & Bandfield, 2006; McLennan et al., 2005; Morris et al., 2006).

A number of different scenarios have been proposed to explain the origin of the Burns formation bedrocks (Berger et al., 2009; McLennan et al., 2005; McCollom & Hynek, 2005; Niles & Michalski, 2009; Squyres et al., 2004; Squyres, Knoll, et al., 2006; Tréguier et al., 2008). In one proposed scenario (hereinafter referred to as the sedimentary-evaporite scenario), the deposits are inferred to have formed through evaporative cementation of chemically altered basaltic mud on the margins of a playa lake, followed by erosion and redeposition in an interdune-sand sheet environment and then by diagenetic alteration (Grotzinger et al., 2005; Hurowitz & Fischer, 2014; McLennan et al., 2005; Squyres et al., 2004; Squyres, Knoll, et al., 2006; Tosca et al., 2005). This scenario invokes a sequential series of events that included (1) chemical alteration of basalt to remove ~55% of the divalent cations (Fe, Mg, and Ca); (2) infiltration of the altered basalt by acidic, sulfate-rich fluids, followed by evaporation of the fluids to precipitate Mg-, Fe-, and Ca-sulfate minerals; (3) erosion of these materials as sulfate-cemented silicilastic sand grains and transport to their present location by wind and water; and (4) diagenetic alteration of the sediments during one or more episodes of groundwater infiltration at their present location that resulted in dissolution of some minerals, precipitation of other minerals that cemented the sand grains, and late-stage diagenetic formation of the hematite spherules (Grotzinger et al., 2005; McLennan et al., 2005; Squyres, Knoll, et al., 2006).

Other scenarios propose that the sulfur component was added to pristine basalt from atmospheric or volcanic sources (Berger et al., 2009; McCollom & Hynek, 2005; Niles & Michalski, 2009; Tréguier et al., 2008). In these scenarios, SO_2 (or SO_3) derived from the atmosphere or from volcanic vapors combined with water to form sulfuric acid, which then reacted with the basalt to form sulfate minerals and other alteration products such as amorphous silica and phyllosilicates. Since the evidence indicates that the framework sediments of the bedrocks were deposited in their present location as sulfate-cemented siliciclastic sand grains (Grotzinger et al., 2005; McLennan et al., 2005; Squyres, Knoll, et al., 2006), these scenarios would require that the addition of the sulfur component from atmospheric or volcanic sources took place prior to deposition of the sediments at their current setting, which could have occurred in a location distant from the current setting of the deposits. Whatever the original source of the sulfur component and the sulfate-cemented sand grains, once deposited at Meridiani, the sediments must have been subjected to fluid infiltration and diagenetic processes as described by McLennan et al. (2005).

A key point of divergence among these various models is the processes and setting that led to the initial formation of the sulfate-cemented sand grains. In particular, one critical factor that differentiates the proposed scenarios is the presumption of whether or not additional elements were added to the precursor basaltic

materials along with the sulfur component. In the sedimentary-evaporite scenario, several elements (primarily the divalent cations Fe, Mg, and Ca) were presumed to be first transported out of the basaltic precursor and then transported back into the materials together with sulfate by infiltrating groundwater, which then precipitated out as sulfate minerals during evaporation of the fluids (e.g., Squyres et al., 2004; Squyres, Knoll, et al., 2006; Tosca et al., 2005). To be consistent with the current basalt-like chemical composition of the deposits, this scenario would require that the amounts and relative proportions of the cations removed from the original basalt and subsequently added back into the deposits by the evaporating fluids must have been nearly identical. Conversely, scenarios involving the addition of the sulfur component from atmospheric or volcanic sources presume that only a sulfur component was added to the original basalt, with no concurrent addition or depletion of other chemical elements. The latter set of models are thus closed to the mobilization of elements other than S (plus some O to oxidize Fe to their current mostly ferric state; Morris et al., 2006) during the initial stage in formation of the sediments, so that the original sulfate-cemented sand grains would retain their original elemental composition from the precursor basalt for elements other than S and O.

In each of these scenarios, interaction of the original basaltic materials with acidic, sulfate-rich fluids is a key component in the formation of the bedrocks. In the sedimentary-evaporite scenario, acidic fluids were presumably involved in the initial removal of the divalent cations from the precursor basalt, and evaporation of acid-sulfate fluids is proposed to be the source of sulfate minerals in the original sand grains (Squyres et al., 2004; Squyres, Knoll, et al., 2006; Tosca et al., 2005). In other scenarios, sulfur is originally introduced to the deposits as sulfuric acid derived from atmospheric or volcanic sources (Berger et al., 2009; McCollom & Hynek, 2005; Niles & Michalski, 2009; Tréguier et al., 2008). Finally, the identification of jarosite in the current deposits implies that conditions were at least moderately acidic during diagenetic alteration of the sediments, since acidic conditions are required for this mineral to precipitate (Klingelhöfer et al., 2004; Morris et al., 2006).

3. Conceptual Approach to Assess Mobility

Mobility of phosphorous in the Burns formation is assessed primarily through comparison of the relative abundances of P and Ti in the bedrocks with examples of Martian basalts. Two primary processes are likely to have been the dominant influences on the absolute abundances of these elements and on P:Ti ratios in the bedrocks: igneous fractionation during crystallization of the precursor basaltic melt and subsequent mobilization by fluids during aqueous alteration (Figure 2). During fractional crystallization of magma, P and Ti behave similarly as incompatible elements. As crystallization progresses, these elements accumulate in the residual melt and should maintain a constant P:Ti ratio that reflects the original melt composition (Baratoux et al., 2014; Ming et al., 2008). As a consequence, basalts derived from a common source may have variable abundances of P and Ti owing to varying degrees of crystallization, but should maintain a constant P:Ti ratio (green dashed arrow in Figure 2). Of course, processes such as magmatic mixing or incorporation of wall rock can cause P:Ti ratios to vary from the initial melt compositions, and such processes have been invoked to explain the occurrence of some high P basaltic rocks in Gusev crater (Usui et al., 2008).

Subsequent alteration of basalts by aqueous fluids can cause the abundances of P and Ti, as well as the P:Ti ratios, to diverge from their original igneous values. Titanium is commonly used as a reference element to assess the immobility of other elements during alteration because it tends to be highly immobile over a broad range of geologic conditions (e.g., Crovisier et al., 1987; Markússon & Stefánsson, 2011; McCollom, Robbins, et al., 2013; Papike et al., 1991; Ruff et al., 2014; Yen et al., 2017; Zolotov & Mironenko, 2016). If P is similarly immobile during aqueous alteration, the P:Ti ratios are expected to remain constant. Nevertheless, the absolute abundances of P and Ti may passively increase or decrease even when they are immobile as other elements are transported into or out of the rocks (red dashed line in Figure 2). Conversely, if P is transported into or out of the rocks by aqueous fluids while Ti remains immobile, the P:Ti ratio will either increase or decrease depending on whether P is gained or lost from the solid materials (black arrows in Figure 2).

The P:Ti ratio can also diverge from the original igneous values during alteration if Ti is mobilized. Although Ti is essentially immobile in most geologic environments, there are some circumstances under which it can become mobile, including metamorphic temperatures and pressures, very high or low pH (<2 or >12),

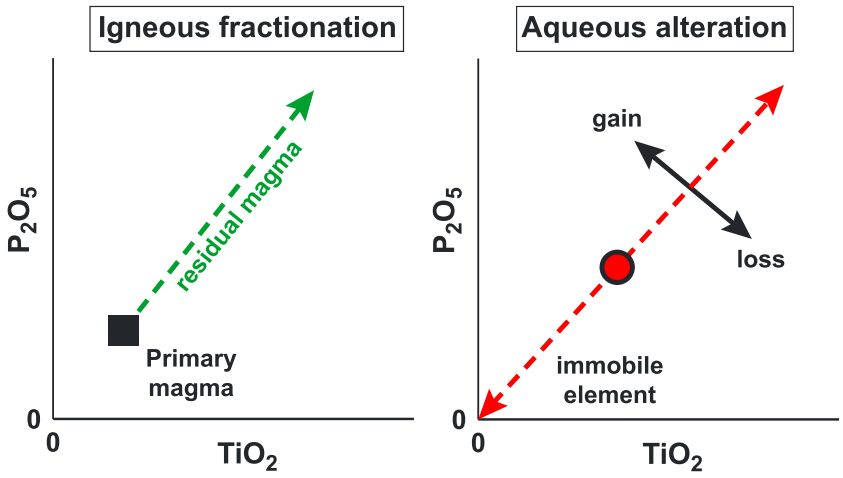

Figure 2. Schematic diagrams illustrating expected trends for P as a function of Ti during igneous fractionation and aqueous alteration. (left) During igneous fractionation, crystallization will cause the abundances of the incompatible elements P and Ti to increase in the residual magma relative to the composition of the primary magma (green arrow), but the P:Ti ratio should remain constant. (right) During aqueous alteration, the P:Ti ratio should remain constant if P is immobile (red dashed line), as long as the alteration occurs under conditions where Ti is also immobile. However, the absolute abundances of both elements may passively increase or decrease along a line of constant P:Ti ratio owing to the transport of other elements into or out of the rocks (red dashed line). If P is transported into the rocks and precipitates as secondary minerals, the increase in the abundance of P relative to Ti will result in higher P:Ti ratios and values that plot to the left of the expected trend for immobility. Conversely, mobilization of P out of the rocks during alteration will result in lower P:Ti ratios that plot to the right of the immobile trend.

areas with extremely high fluid fluxes such as lateritic soils, or settings with high concentrations of complexing agents such as F^- or organic matter (e.g., Cornu et al., 1999; Crossley et al., 2017; Galvez et al., 2012; McHenry, 2009; Van Baalen, 1993). Even in these cases, however, redistribution of Ti generally occurs on relatively small spatial scales, and transport of Ti over distances of more than a few meters appears to be very rare (Van Baalen, 1993).

The approach taken in this study is to compare the abundances of P and Ti and the P:Ti ratios in the Burns formation bedrocks with representatives of Martian basalt compositions. Values that lie outside the expected trends for igneous fractionation and immobility during alteration will be an indication that P (or Ti) has been mobilized at some point during formation of the bedrocks. Conversely, compositions that are consistent with these trends are an indication that little or no mobilization of these elements has occurred.

4. Methods and Data Sources

4.1. Martian Basalt Data

Data for Martian samples were compiled from measurements made by APXS instruments onboard the Pathfinder, Opportunity, and Spirit rovers (Gellert et al., 2006; Rieder et al., 2004; Wänke et al., 2001). A spreadsheet containing all data compiled for this study is provided in Data Set S1. The data for Opportunity and Spirit were downloaded from the NASA Planetary Data System website in October, 2014. Chemical data for the Spirit and Opportunity rovers are derived from measurements made using the APXS and processed with the fit program, method, and calibration parameters described in Gellert et al. (2006). Data for Pathfinder were taken from the summary provided by Wänke et al. (2001). Because the sedimentary deposits within Gale crater that are currently being investigated by the Curiosity rover have a complex history that includes erosion, transport, and diagenetic processes, which may have affected the distribution of P and Ti, they were not included in the reference set intended to represent relatively unaltered Martian basalt compositions. Mobility of P in Gale crater is undergoing evaluation by other workers (e.g., Berger et al., 2016; Yen et al., 2017).

For the Opportunity data, all measurements of bedrocks completed through sol 2515 (Luis de Torres) were included in the database, except for the sample Penrhyn obtained on sol 1843 that exhibited anomalous values for several elemental oxides including Fe and Si. The data up through sol 312 reflect bedrock

compositions in the vicinity of the Opportunity landing site including Eagle and Endurance craters, while the remaining data were acquired during a several kilometer traverse across the Meridiani plains that included observations within Victoria crater (Arvidson et al., 2006, 2011). Two basaltic rocks encountered on Meridiani Planum, Bounce Rock and Marquette, were also included in the compilation and used as additional reference points for interpretation of the Burns formation data. Although Bounce Rock was found next to Eagle crater at Meridiani, it is likely to be ejecta from a nearby crater such as Bopolu (Arvidson et al., 2011) and does not necessarily represent the basaltic source material for the Burns formation deposits. The Opportunity data include only those chemical compositions of bedrock acquired following treatment by the Rock Abrasion Tool (RAT) to remove dust deposits and surface alteration. The Spirit rover database includes a representative suite of 89 measured rock compositions plus the Paso Robles class soils (Gellert et al., 2006; Ming et al., 2006, 2008; Yen et al., 2008). The database includes representatives of all the rock classes at Gusev as defined by Gellert et al. (2006); Squyres, Arvidson, et al. (2006); and Ming et al. (2006, 2008). For those sample sites where the rocks were abraded or brushed by the RAT prior to APXS analysis, those data were used in the database. However, because these data were not available for all sample sites, some unbrushed samples were included in the Gusev database. These unbrushed samples may include a dust component and surface alteration that affect the measured compositions to some degree (e.g., Hausrath et al., 2008; Hurowitz et al., 2006). However, it was determined that including the broadest and most representative diversity of sample compositions outweighed the degree of uncertainty introduced by including the unbrushed samples, particularly since some rock classes are not represented by abraded or brushed samples. The list of samples included in the database can be found in Data Set S1.

Bulk compositional data were also compiled for a suite of 23 basaltic Martian meteorites. The meteorite data were obtained from the compilations of Lodders (1998) and Treiman and Filiberto (2015) with additional data from Barrat et al. (2002) and Agee et al. (2013). Meteorites included in the compilation are Zagami, Los Angeles, Shergotty, EET79001A and EET79001B, NWA7304, NWA5789, NWA6234, NWA4925, NWA5990, NWA5990, NWA5298, NWA1068/1110, ALH77005, LEW88516, DaG 476, DaG 489, SAU 005, Dhofar 019, Dhofar 378, Larkman Nunatak 06319, Yamato 980459, and Ksar Ghilane 002. Chemical compositions for these meteorites are included in Data Set S1.

4.2. Terrestrial Analog Data

To provide additional perspective, the fate of P was also investigated at Cerro Negro (CN) volcano, Nicaragua, which is being studied as a terrestrial analog for acid-sulfate alteration of basalt in fumarolic environments on Mars (Hynek et al., 2013; McCollom, Hynek, et al., 2013). As part of a broader study, the bulk chemical compositions of 76 altered basalt cinder deposits and several examples of pristine basalt were determined, including samples collected in 2008 and 2015 (see McCollom, Hynek, et al., 2013, for detailed description of sample localities). Analyses were conducted on bulk samples at Activation Laboratories Ltd. (Ontario, Canada) using a combination of X-ray fluorescence, inductively coupled plasma-optical emission spectroscopy, instrumental neutron activation analysis, and infrared detection during combustion (for SO_4). The data discussed here include analyses reported in McCollom, Hynek, et al. (2013) supplemented with more recent data. The CN data are also supplied in Data Set S2.

4.3. Laboratory Experiments

A set of laboratory experiments were also conducted to examine the fate of P during acid-sulfate alteration of basalts with elevated abundances of this element. For the experiments, apatite was combined with fresh CN basalt to reach a bulk P_2O_5 abundance in the solids of about 1 wt%, a level comparable to that of the Meridiani deposits and many of the basaltic rocks at Gusev crater. A series of experiments were conducted that encompassed a range of durations (11–30 days) and fluid:rock ratios (1–3 by mass). However, since these experiments produced very similar results, for brevity, only one of the experiments (ADSU17) is reported in detail here. Experiment ADSU17 was performed and analyzed with methods previously used to investigate acid-sulfate alteration of CN basalt as described in McCollom, Robbins, et al. (2013). Detailed descriptions of the experimental and analytical procedures are provided as supporting information. Briefly, basalt cinders from CN (6 g, 2–10 mm diameter), apatite (109 mg), and 1 M sulfuric acid (18.8 g) were placed in a Teflon-lined acid-digestion bomb (Parr Instruments, Inc.) and heated at 150 °C for 27 days. Following incubation, the reactor was cooled to room temperature and opened to recover the reacted solids. Upon opening, the reacted cinders were coated with white material composed largely of silica gel (McCollom, Robbins, et al., 2013).

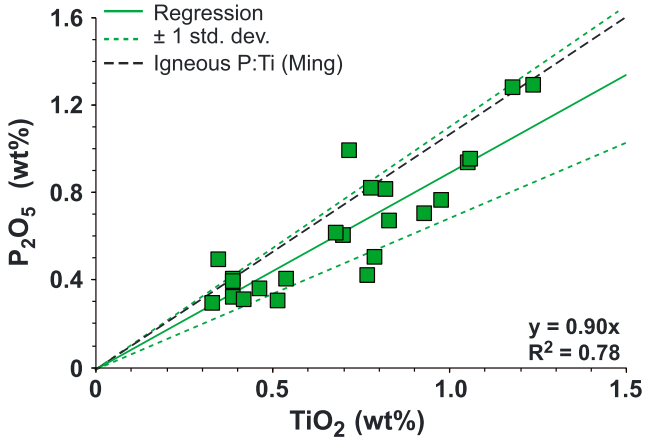

Figure 3. Abundances of P_2O_5 and TiO_2 in basaltic meteorites. The solid green line represents a linear regression to the data with regression parameters shown, which yields a slope that is virtually identical to the average P_2O_5:TiO_2 ratio. The green dashed lines represent ±1 standard deviation from the average P_2O_5:TiO_2 ratio. The black dashed line represents the P:Ti ratio inferred for igneous fractionation by Ming et al. (2008).

The cinders were rinsed with ethanol to remove this gelatinous material, and then allowed to dry in a fume hood. Solid reaction products precipitated on the reacted cinders were analyzed by X-ray diffraction (XRD) and scanning electron microscopy equipped with electron-dispersive X-ray spectroscopy (EDS). Additional characterization of the solid reaction products was performed using Raman spectroscopy and Mössbauer (MB) spectroscopy.

5. Phosphorous in Martian Rocks

5.1. Phosphorous Trends in Martian Basalts

To provide context for evaluation of P mobility in the Burns formation deposits, we first review the occurrence of P in basaltic meteorites and in basaltic Martian rocks investigated in situ by rovers at Gusev crater and elsewhere. These samples provide the best opportunity to constrain the possible abundances of P and Ti in the precursor basalt for the Burns formation bedrocks, and together they provide a contextual framework to interpret the measured abundance of P in the bedrocks.

5.1.1. Martian Meteorites

The measured abundances of P_2O_5 and TiO_2 in basaltic Martian meteorites are displayed in Figure 3. Baratoux et al. (2014) observed that these elements maintain an approximately constant ratio in the basaltic shergottites, with an average TiO_2:P_2O_5 ratio of 1.151 ± 0.265 (1σ) (which translates to an average P_2O_5:TiO_2 ratio equal to 0.87; note that here and throughout this report ratios refer to relative weights and not molar proportions). This value agrees with the compilation of basaltic meteorites included here, which have an average P_2O_5:TiO_2 ratio of 0.89 with a standard deviation of 0.21. The black dashed line in Figure 3 represents the igneous fractionation line for Martian basalts proposed by Ming et al. (2008), which corresponds to a P_2O_5:TiO_2 ratio of 1.08. The Ming et al. line was derived from meteorite data reported by Longhi et al. (1992), but the compilation of meteorite data shown in Figure 3, which includes more recent information, suggests a trend with a somewhat lower P_2O_5:TiO_2 ratio. The scatter around the general linear trend may indicate that the meteorites represent residual melts derived from primary magmas that have somewhat different P_2O_5:TiO_2 ratios, but the scatter could also arise from other magmatic processes or from errors in estimating the P_2O_5 and TiO_2 contents of the meteorites. In any event, most of the data appear to be consistent with igneous fractionation from melt sources containing a very narrow range of P_2O_5:TiO_2 ratios near 0.89.

5.1.2. Gusev Crater

The rocks examined by the Spirit rover in Gusev crater have basaltic compositions, although many of them have experienced some degree of surface weathering or alteration (Ming et al., 2006, 2008; McSween et al., 2008; Squyres, Arvidson, et al., 2006). The measured abundances of P_2O_5 in the Gusev rocks as a function of TiO_2 are displayed in Figure 4, where the data have been partitioned into rock classes as defined by Gellert et al. (2006); Squyres, Arvidson, et al. (2006); and Ming et al. (2006, 2008). Also shown in the figure are measured compositions of the Paso Robles class soils, two of which have highly elevated P abundances (Yen et al., 2008).

Most of the basaltic rocks at Gusev have P_2O_5 abundances between 0.45 and 1.63 wt%, and also cluster along the line of constant P:Ti ratio proposed for igneous fractionation by Ming et al. (2008), which is shown as the black dashed line in Figure 4a. It appears likely therefore that the P contents of this group of rocks are consistent with primary igneous processes involving melting of Martian mantle and subsequent fractionation during magma crystallization. On the other hand, the rocks of the Wishstone, Watchtower, and Independence classes contain higher P_2O_5 abundances, and most of the rocks in these classes also have substantially higher P_2O_5:TiO_2 ratios than expected for igneous fractionation (Ming et al., 2008; Usui et al., 2008). The P contents and elevated P_2O_5:TiO_2 ratios of the members of these three rock classes suggest that they have been enriched in P through either magmatic or aqueous processes (Ming et al., 2008; Usui et al., 2008). Geochemical analysis also indicates that a Ca-rich phosphate mineral has weathered out of the surface rind of members of the high-P Wishstone and Watchtower class rocks (Hurowitz et al., 2006). As a

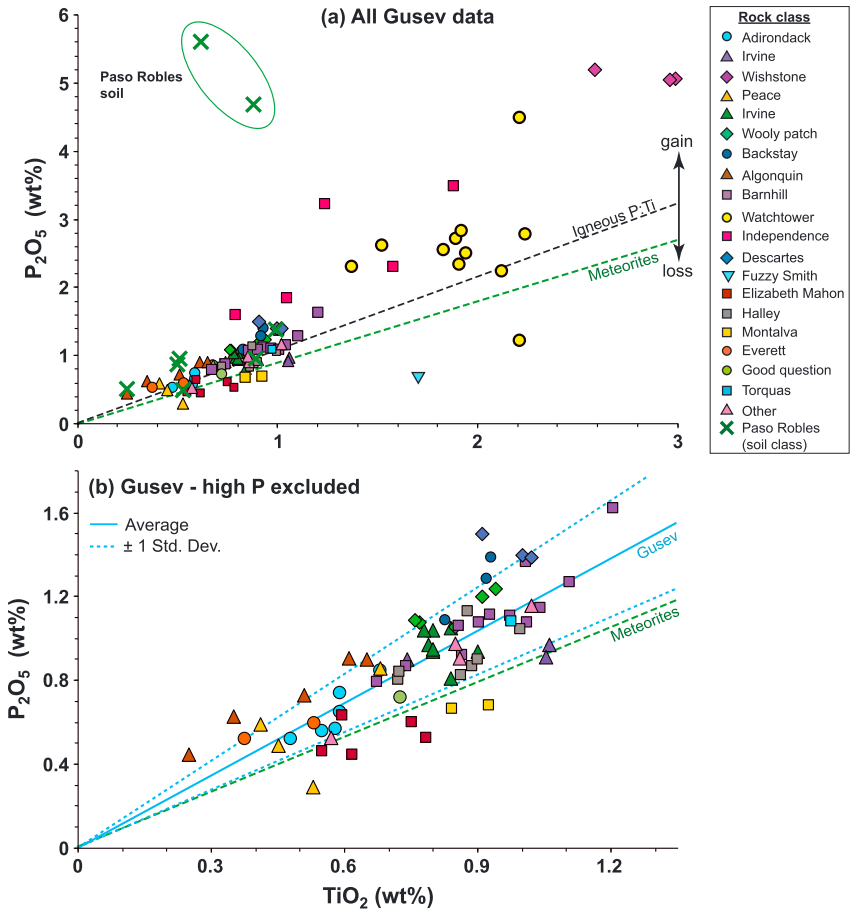

Figure 4. (a) Abundances of P_2O_5 and TiO_2 in rocks at Gusev crater measured by the Spirit rover, with data separated into rock classes. Also shown are compositions of Paso Robles class soils (Yen et al., 2008). The green dashed line represents the average P_2O_5:TiO_2 ratio for meteorites, while the black dashed line represents the P:Ti ratio expected for igneous fractionation proposed by Ming et al. (2008). The green oval in the upper left highlights measurements for the Paso Robles soil. Figure adapted from Ming et al. (2008). (b) Gusev data with high P rocks from the Wishstone, Watchtower and Independence classes excluded. The solid blue line represents the average P_2O_5:TiO_2 ratio for the Gusev samples (excluding the high P classes), and the blue dashed lines are ±1 standard deviation from this average. A linear regression of the data shown in (b) results in a trend that overlaps the average line, with a slope of 1.15, a *y* intercept of 0.01, and an $R^2 = 0.65$, which would be consistent with an igneous fractionation line with a constant P_2O_5:TiO_2 ratio that passes through the origin (Figure 2).

consequence, the measured compositions of the rocks in the Wishstone, Watchtower, and Independence classes are unlikely to be representative of igneous fractionation trends for most Martian basalts. The rock named Fuzzy Smith has a somewhat anomalous composition compared to the other Gusev samples, with low P_2O_5 coupled to a relatively high TiO_2 abundance (Figure 4a). One proposed explanation for the low P_2O_5:TiO_2 ratio observed in this rock is dissolution and leaching of P-bearing minerals by acidic solutions under open-system conditions (Ming et al., 2008).

When the high P rock classes and Fuzzy Smith are excluded, the remaining rock compositions conform to a positive linear trend with an average P_2O_5:TiO_2 ratio of 1.17 and a standard deviation of 0.24 (Figure 4b). This average is slightly higher than the P_2O_5:TiO_2 ratio for the igneous fractionation trend proposed by Ming et al. (2008) (=1.08). Nevertheless, the linear trend for this suite of samples appears to be consistent with igneous fractionation from primary melts containing the same or very similar P_2O_5:TiO_2 ratios. In general, the unbrushed rock samples have a slightly lower range of P_2O_5:TiO_2 ratios than the RAT-treated and brushed samples (Figure 5), which might reflect a minor contribution from dust or surface alteration (e.g., Hurowitz et al., 2006). However, there is considerable overlap among samples from each treatment type.

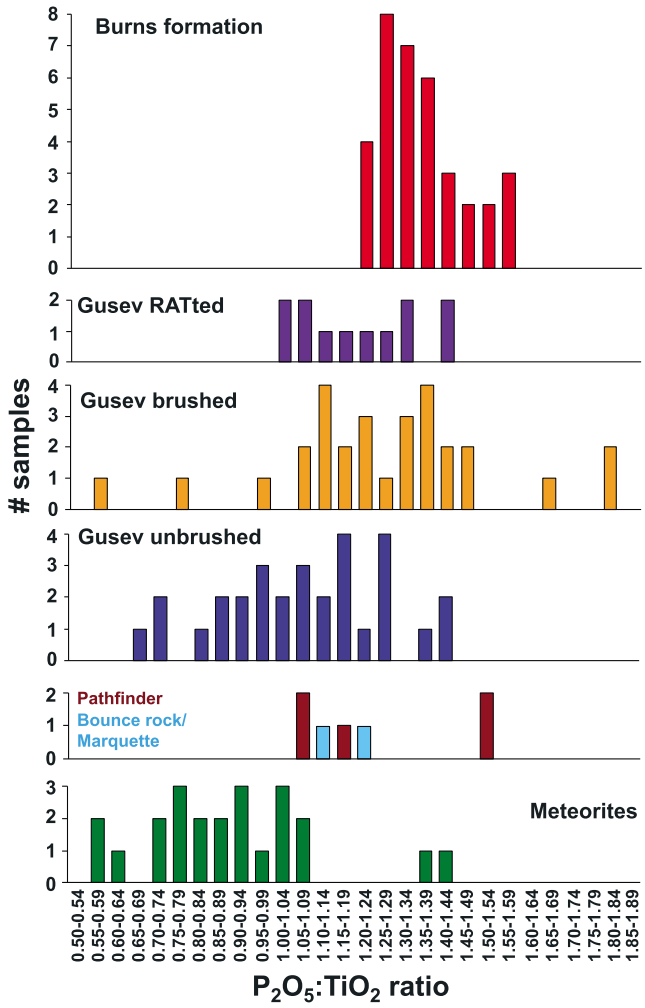

Figure 5. Histograms of P_2O_5:TiO_2 ratios for Burns formation bedrocks and basaltic Martian rocks. The basaltic rocks from Gusev are divided by sample treatment (abraded by the RAT, brushed, or unbrushed), and samples from the high P Wishstone, Watchtower, and Independence classes have been excluded.

Basalts from the Pathfinder landing site as well as Bounce Rock and Marquette from the Opportunity site also have measured abundances of P_2O_5 and TiO_2 that cluster within this suite of Gusev basalts (Figure S1), as well as similar P_2O_5:TiO_2 ratios to the RAT abraded and brushed Gusev samples (Figure 5).

Although there is some overlap, the P_2O_5:TiO_2 ratios for the Gusev rocks are generally higher than those of the basaltic Martian meteorites, which have an average ratio of 0.89 (Figure 5). This discrepancy could be an indication that the Gusev basalts (as well as Bounce Rock/Marquette and rocks from the Pathfinder landing site) are derived from primary melts that have higher P_2O_5:TiO_2 ratios than those of most Martian meteorites. An alternative possibility is that the primary melts for all of the basaltic rocks at the rover sites initially had lower P_2O_5:TiO_2 ratios similar to the meteorites, but were systematically enriched in P by magmatic or aqueous processes like those proposed to account for the high P rocks at Gusev (e.g., Ming et al., 2008; Usui et al., 2008). However, this seems like an unlikely possibility since it would require very similar levels of enrichment across a broad suite of samples. More likely, the data for Gusev and other rover samples reflect igneous fractionation from melt reservoirs that have somewhat higher initial P_2O_5:TiO_2 ratios than most basaltic meteorites.

Figure 4a also shows P_2O_5 and TiO_2 measurements for the Paso Robles class soils. The soils in this class are a group of sulfur-rich, light-toned, unconsolidated deposits encountered by the Spirit rover during its traverse across the Columbia Hills (Yen et al., 2008). Among the soils in the Paso Robles class (green crosses in Figure 4a), most samples have P_2O_5 abundances and P_2O_5:TiO_2 ratios that are similar to the majority of Gusev basalt samples, and cluster close to the line defining the expected igneous fractionation trend for pristine Martian basalt. However, the light-toned soil named Paso Robles, which was exposed by the rover's wheels during its traverse, exhibits anomalously high P_2O_5 abundances not present in other members of the class (upper left corner of Figure 4a; Yen et al., 2008). The Paso Robles soil sample also contains elevated SO_3 and has been interpreted to be composed predominantly of a mixture of basaltic soil, amorphous silica, Fe- and Mg-bearing sulfates, and a Ca-phosphate mineral (Yen et al., 2008). However, Fe-phosphate and Ca-sulfate minerals could also be present (e.g., Lane et al., 2008; Ming et al., 2006).

Because the Paso Robles soil occurs in close proximity to rocks of the Wishstone and Watchtower classes that have elevated P abundances, a local source has been inferred for the elevated P in the Paso Robles soil (Yen et al., 2008). However, the soil has a substantially higher P_2O_5:TiO_2 ratio than the surrounding rocks (Figure 4a), suggesting that mixing of fine material eroded from nearby rocks into Martian soil cannot fully account for the enrichment. The presence of elevated SO_3 and sulfate minerals in the Paso Robles class soils suggests that they may have formed under acidic conditions in a fumarolic or hydrothermal environment (Yen et al., 2008). In this acidic, sulfate-rich environment, P may have been transported into the Paso Robles soil by aqueous solutions during weathering of adjacent P-rich rocks (Hurowitz et al., 2006; Ming et al., 2006, 2008).

5.2. Assessment of P Mobility in the Burns Formation

Having established a baseline for the abundance of P and Ti in martian basalts, the abundances of these elements in the Burns formation can be examined. The measured abundances of P_2O_5 and TiO_2 in the layered sulfate-rich bedrocks of the Burns formation are displayed in Figure 6a. The Burns formation bedrocks encompass a narrow range of P_2O_5 compositions between 0.97 and 1.17 wt% and also have a narrow range of measured TiO_2 compositions between 0.65 and 0.90 wt% (Figure 6a). Given the relatively large

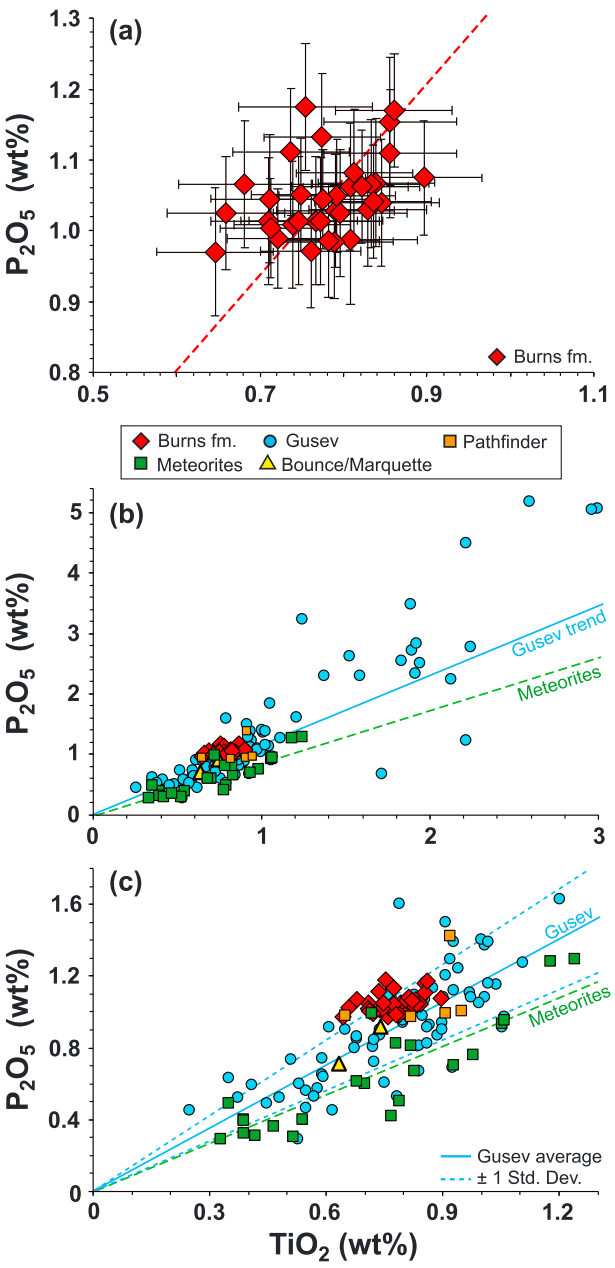

Figure 6. Abundances of P_2O_5 and TiO_2 in bedrocks of the Burns formation at Meridiani Planum and other Martian samples. (a) Measured compositions of Burns formation bedrocks, with reported analytical uncertainties shown by black bars. The red dashed line represents a linear regression constrained to pass through the origin. (b) Comparison of the Burns formation bedrocks with Martian basaltic rocks, including Martian meteorites, rocks from Gusev crater analyzed by the Spirit rover, Bounce Rock and Marquette from Meridiani Planum, and rocks from the Pathfinder landing site. (c) Similar to (b), but with scale expanded to focus on the majority of the data. In (b) and (c), the green dashed line corresponds to the average P_2O_5:TiO_2 ratio for basaltic Martian meteorites, while the solid blue line represents the average P_2O_5:TiO_2 ratio for Gusev basalts, with the ±1 standard deviation envelope outlined by dashed lines. The Gusev average excludes the high P basalt samples from the Wishstone, Watchtower, and Independence classes. For all rover data, measurement uncertainties are similar to the size of the symbols in (b) and slightly larger than the symbols in (c).

uncertainty associated with the measurements (Figure 6a), these values are only barely distinguishable from one another. The Burns bedrocks have an average P_2O_5:TiO_2 ratio of 1.35 with a standard deviation of 0.10.

The abundances of P_2O_5 and TiO_2 in the Burns formation are compared with the reference set of Martian basalts in Figures 6b and 6c. The compositions of the Burns formation bedrocks cluster close to the main group of Gusev basalts as well as basaltic rocks from the Pathfinder and Opportunity sites. The Burns formation rocks also have P_2O_5:TiO_2 ratios similar to those observed for basaltic rocks by the rovers (Figure 5). The Burns bedrock compositions are particularly close to those of several members of the Clovis, Wooly Patch, Barnhill, and Backstay classes from Gusev, rocks from the Pathfinder site, and Bounce Rock from the Opportunity site (Figures 5 and 6c; see also Figure S2). Additionally, the Gusev samples that are closest in P_2O_5 and TiO_2 abundances to the Burns formation rocks are RAT-treated and brushed samples (see Figures 5 and S4). Conversely, the abundance of P and the P_2O_5:TiO_2 ratios in the Burns formation rocks are substantially higher than most of the basaltic meteorites (Figures 5 and 6), although the P_2O_5:TiO_2 ratios are similar to two of the meteorites (DaG 389 and NWA 5990).

The most straightforward explanation of the data shown in Figures 5 and 6 is that the Burns formation rocks have maintained the abundances of P_2O_5 and TiO_2 from their original basaltic precursor and have experienced little or no mobilization of these elements subsequent to crystallization of the basalt. The Burn formation rocks contain abundances of P_2O_5 and TiO_2 as well as P_2O_5:TiO_2 ratios that are well within the range of observed values for basaltic rocks from the rover landing sites. The measured compositions of the Burns formation bedrocks are therefore consistent with igneous fraction trends defined by in situ measurements of Martian basalts. The Burns bedrocks have P_2O_5:TiO_2 ratios that are slightly higher than the Gusev average, but this is not necessarily an indication that there has been any addition of P (or loss of Ti) to the bedrocks since there are several basaltic rocks that have similar measured ratios (Figure 5). Consequently, the precursor basalt for the Burns formation may simply have solidified from a melt with a slightly higher-than-average P_2O_5:TiO_2 ratio similar to that evident in several other basalts. Although the absolute abundances of P_2O_5 and TiO_2 expressed as weight percent in the Burns formation bedrocks have been diluted from their original values by the addition of SO_3 to the deposits (i.e., red dashed line in Figure 2), the basis for the interpretation that P and Ti were essentially immobile is not changed if compositions are normalized to account for the added sulfur contents (see Figure S3). Notably, this interpretation would imply that the precursor basalt for the Burns formation crystallized from a melt with a P_2O_5:TiO_2 ratio similar to that of basalts present at the rover landing sites, but significantly higher than most basaltic meteorites (Figure 5).

The data do not, however, entirely eliminate the possibility that a small amount of element mobility has occurred. It is possible that the precursor basalt originally had a lower P_2O_5:TiO_2 ratio that was more similar to that of the average value for Gusev basalts or for basaltic meteorites (Figure 6c), and the materials were subsequently enriched in P (or

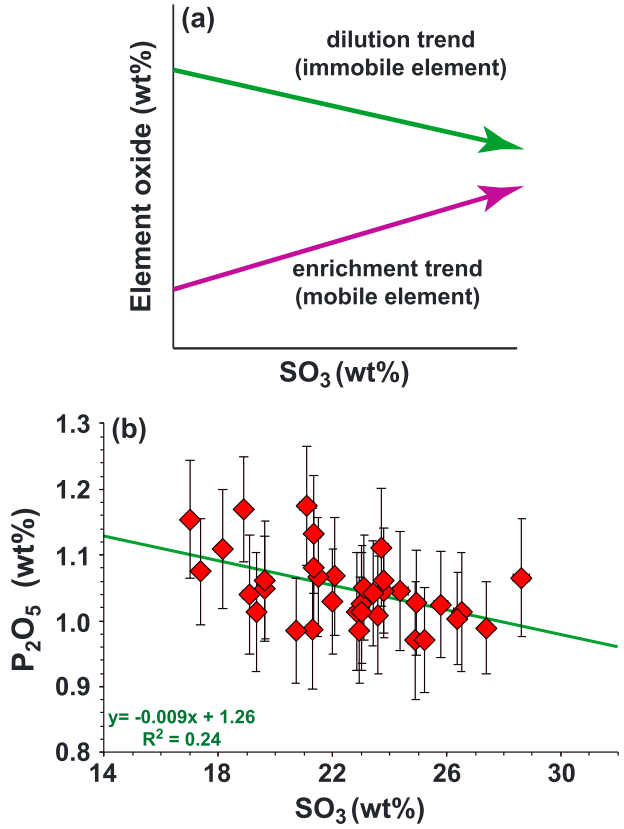

Figure 7. Abundance of P_2O_5 as a function of SO_3 in Burns formation bedrock at Meridiani Planum. (a) Schematic diagram illustrating expected trends for elements that were immobile during addition of the sulfur component (dilution trend) or mobilized into the deposits along with the sulfur component (enrichment trend). (b) Measured P_2O_5 and SO_3 abundances. The green line represents a linear regression to the data, with fit parameters shown. The bars are analytical uncertainties for P_2O_5; uncertainties for SO_3 are approximately the size of the symbols.

depleted in Ti) through secondary magmatic processes or aqueous alteration. Even in this case, however, the amount of P or Ti mobilized would only represent a relatively small fraction of the total amount of these elements present in the rocks. For instance, addition of only 0.14 wt% P_2O_5 to a rock containing 0.91 wt% P_2O_5 and 0.78 wt % TiO_2 would be sufficient to shift the P_2O_5:TiO_2 ratio from the average Gusev value to the average Burns formation value. Slightly higher amounts of P would have to have been added if the original composition was closer to that of the meteorite average, but would still represent a relatively minor fraction of the total content. In any event, there is no indication for substantial enrichments in P like that which is evident in the Paso Robles soil or members of the Wishstone, Watchtower, and Independence rock classes at Gusev, nor for a significant loss of P like that observed for Fuzzy Smith (Figure 4a). Furthermore, it is worth emphasizing that no mobilization of either P or Ti is required to explain the abundances of the elements or the P_2O_5:TiO_2 ratios in the Burns formation rocks since their compositions can be fully explained without invoking mobilization (Figures 5 and 6).

It is also within the realm of possibility that a large proportion of the P from the original precursor basalt was removed at an early stage in the formation of the Burns bedrocks and was then replaced at a later stage, as has been proposed for the divalent cations (Squyres, Knoll, et al., 2006). However, this would require that the amounts of P removed from the rocks and later replaced to be almost identical; otherwise, the present P_2O_5:TiO_2 ratio would not closely resemble those of many Martian basalts. This therefore seems like a rather remote possibility, and unlikely to be the best explanation for the observations.

Owing to their low abundances, the measurements of P_2O_5 and TiO_2 have relatively large uncertainties amounting to approximately 10% of the reported values (Figure 6a). However, even when these uncertainties are taken into account, the abundances of P_2O_5 and TiO_2 and the P_2O_5:TiO_2 ratios remain within the range of values for Martian basalts analyzed in situ by the rovers (note that all of the other rover-based data shown in Figure 6 have uncertainties similar to the Burns formation data). As a consequence, allowance for measurement uncertainties does not invalidate the conclusion that P and Ti were essentially immobile.

An additional constraint on the mobility of P during formation of the Burns bedrocks is provided by assessment of the abundance of P_2O_5 relative to SO_3. The elevated SO_3 in the Burns formation is thought to be the result of the addition of a sulfur component to materials derived from basalt, likely under acidic conditions (e.g., Berger et al., 2009; McCollom & Hynek, 2005; Squyres et al., 2004; Squyres, Knoll, et al., 2006; Tréguier et al., 2008). If P had been transported into the deposits along with the sulfur component (for example, by a process similar to that proposed to account for simultaneous enrichments of SO_3 and P_2O_5 in the Paso Robles soil; Yen et al., 2008), the measured abundance of P_2O_5 would be expected to increase linearly with the abundance of SO_3 (purple arrow in Figure 7a). Conversely, if P was not transported into the deposits along with the sulfur component, the abundance (in wt%) of P_2O_5 in the bedrocks would be expected to decrease with increasing SO_3 owing to passive dilution by the addition of the sulfur component (green arrow in Figure 7a).

As shown in Figure 7b, P_2O_5 exhibits a general trend of decreasing abundance with increasing SO_3. However, the relatively large uncertainty associated with the P_2O_5 measurements makes it difficult to place a high degree of confidence in this trend. Nevertheless, there is no indication for an enrichment trend that would indicate that some PO_4 was transported into the deposits along with the sulfur component, and the trend appears to be consistent with the conclusion that P experienced little or no mobilization during addition of the sulfur component to the basalt precursor.

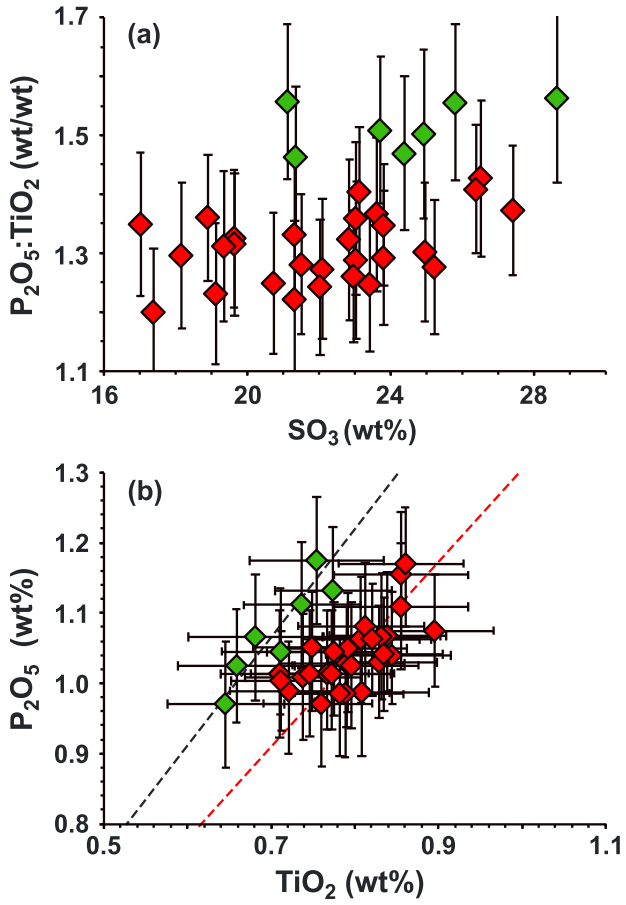

Figure 8. Geochemical trends in the Burns formation with a subset of seven samples with slightly offset compositions plotted separately as green diamonds. (a) P_2O_5:TiO_2 ratio plotted as a function of SO_3. (b) P_2O_5 plotted as a function of TiO_2. The dashed lines represent regression lines constrained to pass through the origin.

Lastly, while the bulk of the measured analyses of Burns formation bedrocks form a tight cluster with compositions indicating their P or Ti were derived primarily from the original basaltic precursor with little or no subsequent mobilization, a small subset of samples have slightly offset compositions that may indicate they have been subjected to additional processes. This subset of seven samples (Guadalupe, Kentucky, Ontario, Millstone, Paikia, Gagarin, and Baltra) appears to form a coherent group with slightly higher P_2O_5:TiO_2 ratios than the other samples (Figure 8). However, the difference is small relative to the analytical uncertainties, so definition of this group is somewhat uncertain. Geochemical trends for this subset parallel those of the other samples (Figure 8). The seven samples in the subset do not exhibit any obvious geographic distribution or physical characteristics that would provide insight into the reason for the offset in P_2O_5:TiO_2 ratios.

As a group, the offset samples contain similar amounts of P_2O_5 to the other samples but have generally lower TiO_2 abundances (Figure 8b), suggesting that the higher P_2O_5:TiO_2 ratios are largely attributable to lower TiO_2 contents. This could be an indication that the offset samples have been slightly depleted in Ti through aqueous alteration at some stage during formation of the bedrocks. However, the offset could also be explained by other factors, such as a slight localized depletion in the abundance of Ti-bearing minerals in some samples, either as a result of processes occurring during magma crystallization or during transport of the materials to their present location. Whatever the cause, the offset requires $<$10% difference in the abundance of TiO_2 among samples. In any case, the presence of a few samples with slightly higher P_2O_5:TiO_2 ratios does not contradict the overall conclusion that P and Ti were essentially immobile throughout formation of the deposits.

6. Examination of P Mobility During Natural and Experimental Acid-Sulfate Alteration of Terrestrial Basalts

The data shown in Figures 5–7 indicate that there has most likely been little or no mobilization of P throughout the development of the Burns formation bedrocks. This result would seem to be inconsistent with the general expectation that P is readily mobilized under acidic conditions, requiring further investigation into factors that might have precluded this element from being transported into or out of the layered sulfate bedrocks as they formed. To gain a better understanding of the factors that control P mobility under acid-sulfate conditions, the fate of P during acid-sulfate alteration of basalt was examined at a terrestrial Mars-analog field site and in laboratory experiments.

6.1. Phosphorous Mobility During Acid-Sulfate Alteration in Fumarolic Environments at Cerro Negro Volcano

Cerro Negro is a small, young cinder cone volcano in Nicaragua where basaltic cinders are actively undergoing acid-sulfate alteration by SO_2-bearing volcanic vapors at several fumaroles (Figure 9; Hynek et al., 2013; McCollom, Hynek, et al., 2013). Fresh CN basalt cinders are composed of phenocrysts of plagioclase, augite, olivine, and opaque minerals embedded within a glassy matrix (McCollom, Hynek, et al., 2013; McCollom, Robbins, et al., 2013). At sites of focused vapor discharge, temperatures can reach above 300 °C with pH approaching 0. In these areas, the cinders are extensively altered, resulting in deposits composed of little more than amorphous silica with trace amounts of barite and Fe- and Ti-bearing oxides/oxyhydroxides. The focused vents are surrounded by much larger areas where vapors permeate diffusively through unconsolidated deposits, providing moist conditions and temperature gradients that range from ambient at the surface to $>$200 °C a few decimeters below the surface (Figure 9b). In these areas, conditions are less strongly acidic, with pH values ranging from 1 to 4, and the cinders have experienced lesser degrees of chemical and mineral alteration.

Figure 9. Examples of fumarolic environments at Cerro Negro volcano. (a) Mound of altered cinders surrounding an active fumarole ("CN4 mound"), with focused venting of volcanic vapors at the top and more diffuse discharge around margins. White patches on the surface are gypsum. Mound is ~12 m across. (b) Trench dug into altered cinder deposits in region of diffuse discharge of steam at site identified as "95 Crater." Note the presence of steam vapors in deeper part of trench. Temperature at the surface is close to ambient but exceeds 200 °C at bottom of trench. Shovel head is 22 cm long. See McCollom, Hynek, et al. (2013) and Hynek et al. (2013) for additional images and descriptions of the sample sites.

Common alteration products in the diffuse areas include amorphous silica, partially altered basaltic glass, Fe-rich natroalunite, and hematite plus other Fe-oxides/oxyhydroxides. In many areas of diffuse discharge, the vapors have transported Ca and SO_4 toward the surface where these elements precipitate as gypsum in the top few centimeters of the deposits as the condensed vapors evaporate. The resulting gypsum deposits form white patches that cover large areas of the surface (e.g., Figure 9a). In most cases, the gypsum precipitates in deposits that have previously undergone extensive mineral alteration and loss of several chemical elements (McCollom, Hynek, et al., 2013).

Figure 10 displays the relative amounts of elements lost or gained from a selected suite of samples from CN that have experienced a range in extent of alteration. The suite of samples shown in this figure does not include those with gypsum precipitates, but similar patterns are observed in areas where gypsum occurs (McCollom, Hynek, et al., 2013). In Figure 10, the enrichment or depletion of elements in the altered deposits relative to pristine basalt is calculated according to the formula:

$$\text{Enrichment/depletion} = (\text{wt\% element/wt\% } TiO_2)_{\text{sample}} / (\text{wt\% element/wt\% } TiO_2)_{\text{basalt}} \quad (1)$$

where Ti is presumed to represent an immobile reference element. Values less than 1 indicate loss of the element relative to pristine basalt, while values greater than 1 indicate enrichment. The figure shows that most elements, including Mg, Fe, Ca, Al, Na, and K, display a systematic depletion relative to pristine basalt, reflecting progressive loss of the elements with increasing degree of acid-sulfate alteration (McCollom, Hynek, et al., 2013). On the other hand, P remains at levels similar to that of pristine basalt in all but the most extensively altered samples. These extensively altered samples contain little more than amorphous silica, native sulfur, barite, and anatase.

Figure 11 shows the abundance of several elements in the CN deposits as a function of TiO_2, with the red dashed lines representing the constant element:TiO_2 ratios that are expected if the element is immobile during alteration (see Figure 2). For Si, many samples plot near the red dashed line, indicating that little or no SiO_2 has been transported into or out of these samples. However, some samples fall above or below the immobile trend, indicating that these samples have experienced a net gain or loss of SiO_2 during alteration. Most of the samples that have gained SiO_2 occur at sites of focused steam venting, and it is likely that the elevated SiO_2:TiO_2 ratios in these samples are attributable to precipitation of amorphous silica from cooling volcanic vapors (McCollom, Hynek, et al., 2013).

The abundances of most other chemical elements lie below the immobile trend for the majority of samples, reflecting extensive loss during alteration. This is seen in Figure 11 for Mg, Fe, and Al, with many samples exhibiting more than 50% loss of these elements relative to pristine basalt. Results for most other elements, including Na, K, Mn, and Cr, are similar (see Data Set S2 for plots of these elements). Calcium is also depleted relative to TiO_2 in most samples, but some samples exhibit variable degrees of enrichment in Ca owing to secondary precipitation of gypsum (Figure 11).

In contrast to most other elements, P exhibits little evidence of transport into or out of the deposits during alteration, except for a few of the most extensively altered samples (Figure 11). As shown in upper right panel of Figure 11, the abundances of P_2O_5 in most samples fall along a positive linear trend as a function of TiO_2,

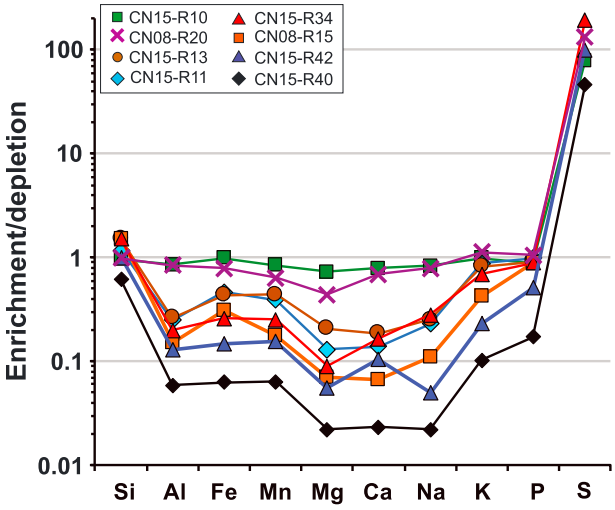

Figure 10. Enrichment (>1) or depletion (<1) of elements in a representative subsample of acid-sulfate altered basaltic cinders at Cerro Negro relative to pristine basalt. In this plot, values >1 indicate enrichment relative to pristine basalt and values <1 indicate depletion. Values for P cluster around 1 except for the most extensively altered samples, indicating little enrichment or depletion of this element relative to pristine basalt for most samples.

with P_2O_5:TiO_2 ratios that are close to the ratios present in the initial basalt. A handful of samples with anomalously high TiO_2 abundances deviate from these trends (purple squares in Figure 11), but these samples represent cases with the most extreme extent of alteration and partial-to-complete removal of all but the least mobile elements (Ti, Zr, and Ba). These samples are composed predominantly of amorphous silica with trace amounts of anatase and barite and may have gained some Ti owing to very high temperatures or pH values near zero. Except for these highly altered samples, the samples exhibit a strong linear correlation that passes through the origin and close to the value for pristine basalt (Figure 11). This trend indicates that P has been largely immobile during alteration of the basalt cinders, except for a small subset of samples that have experienced extensive alteration at high temperature or very low pH.

Owing to the low overall abundance of P in the initial basalt (0.10 wt % P_2O_5), it is difficult to determine the reservoir for this element in the altered cinders. Extensive inspection of grain mounts and polished sections of altered samples did not reveal the presence of any discrete P-bearing mineral such as apatite. The glassy matrix of pristine CN basalt contains ~0.2 wt% P_2O_5 (McCollom, Hynek, et al., 2013) and makes up a large (but undetermined) fraction of the cinders, and this component could potentially account for most (or all) of the P present in the altered cinders. During alteration, the glass phase is the last major component of the cinders to react, and only begins to undergo significant alteration after phenocrysts of plagioclase, augite, and olivine are almost completely decomposed (McCollom, Hynek, et al., 2013; McCollom, Robbins, et al., 2013). Consequently, retention of P in the glass could potentially account for the lack of mobility in all but the most extensively altered samples, since P would not be mobilized until the glass starts to decompose. Alternatively, this element could reside in microphenocrysts of apatite or other P-rich minerals that are embedded within the glass and protected from reaction with the acid-sulfate fluids or could be retained

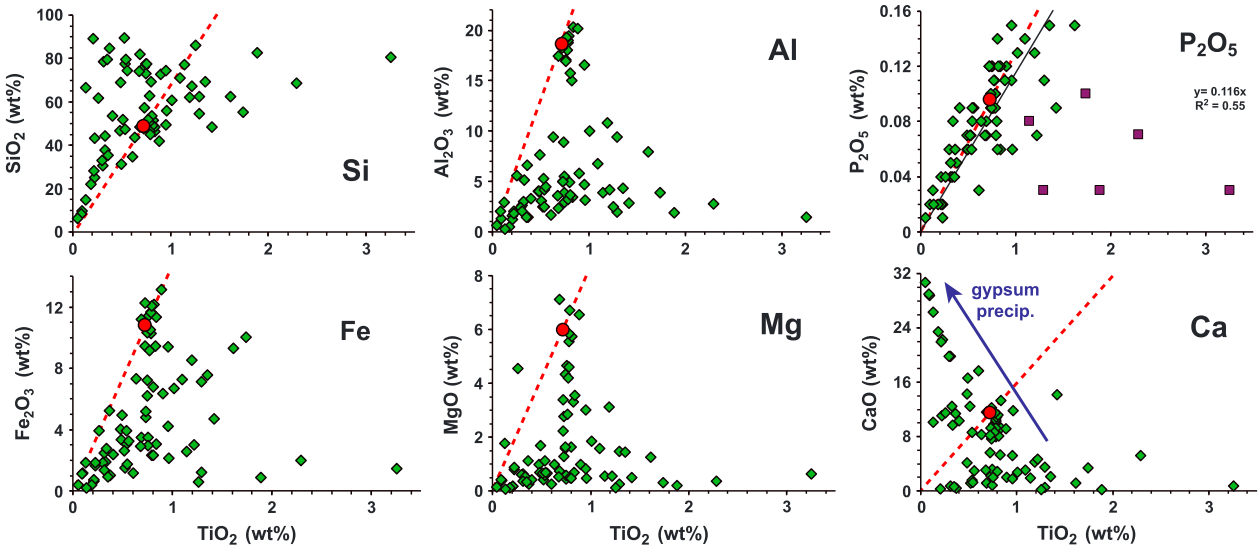

Figure 11. Abundances of selected elements in altered fumarolic deposits at Cerro Negro as a function of TiO_2. The red circles represent the average abundances of the elements in pristine CN basalt, and the red dashed lines represent the constant ratio expected for immobile elements (see text and Figure 2). In the P_2O_5 diagram, the black line is a linear regression to the data, with fit parameters shown. A suite of six samples with anomalously high TiO_2 and/or Zr is plotted separately (purple squares) and were not included in the regression. In the diagram for Ca, the compositions of many samples have been affected by secondary precipitation of gypsum into previously altered deposits (see McCollom, Hynek, et al., 2013).

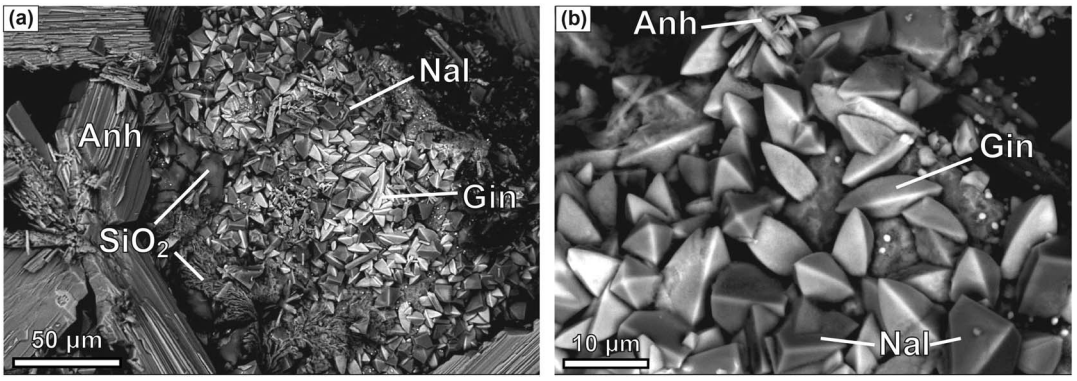

Figure 12. Back-scattered electron images of reaction products from experimental acid-sulfate alteration of CN basalt amended with 1 wt% P_2O_5 (as apatite) in experiment ADSU17. (a) Example of predominant alteration products on the surface of a reacted cinder, including amorphous silica (SiO_2), prismatic anhydrite (Anh), psuedocubic Fe-bearing natroalunite (Nal), and giniite (Gin). (b) Expanded view showing elongated tetragonal morphology of giniite crystals. Small bright spheroids in images are Fe-oxides/oxyhydroxides.

adsorbed to the surfaces of Fe-oxides/oxyhydroxides that are widespread in the altered deposits (e.g., Rampe et al., 2016; Zhao et al., 2014).

6.2. Experimental Alteration of P Enriched Basalt

Because the basalt cinders at CN contain significantly smaller amounts of P than Martian basalts, the fate of P in the altered CN deposits might not be entirely representative of processes occurring during alteration of basalts on Mars. Therefore, laboratory experiments were performed to investigate acid-sulfate alteration of CN basalt in the presence of elevated levels of P. For the experiments, fresh CN basalt cinders were combined with apatite to achieve P_2O_5 levels comparable to those of Martian basalts (1 wt%) and reacted with a sulfuric acid solution in closed-system reactors.

The predominant secondary reaction products in the experiments included amorphous silica, anhydrite, Fe-bearing natroalunite, and Fe-oxides/oxyhydroxides distributed across the surfaces of altered cinders (Figure 12), similar to the products found previous experiments with CN basalts (McCollom, Robbins, et al., 2013). However, addition of apatite to the reactants resulted in the precipitation of an Fe-phosphate mineral along with these other secondary phases. With the exception of the Fe-phosphate, the alteration products closely resemble the alteration mineralogy observed in natural samples from CN (Hynek et al., 2013; McCollom, Hynek, et al., 2013).

The Fe-phosphate occurred as elongated tetragonal crystals that tapered toward the ends (Figure 12b). The Fe-phosphate crystals were widely dispersed across the surfaces of the altered cinders, and in some areas were found in dense aggregates (e.g., Figure 12b). Semi-quantitative analysis of the Fe-phosphate phase by EDS indicated that it contained modest amounts of Al and S in addition to Fe and P (Table S1), indicating that the precipitated mineral occurred as a solid solution containing Al-for-Fe and SO_4-for-PO_4 substitutions. Elemental compositions of the Fe-phosphate minerals determined by EDS suggested that it was likely to be giniite (ideal chemical formula = $Fe^{II}Fe^{III}_4(PO_4)_4(OH)_2 \cdot 2H_2O$). However, it was not present in sufficient quantities to be identifiable in XRD analysis of the bulk reaction products (Figure S5). Therefore, in order to confirm the identity of this phase, samples of pure giniite were synthesized for comparison with the phase produced in the basalt alteration experiments (see the supporting information for a complete description of the synthesis and characterization of the synthetic giniite). Because the Fe-phosphate mineral produced in the basalt alteration experiments included Al and SO_4 substitutions, efforts were made to synthesize and characterize solid solutions of giniite containing these components.

Raman spectra for the synthetic giniites provided a close match to the Fe-phosphates from the basalt experiments, confirming that the experimental products were indeed giniite (Figure 13). In addition, the Raman spectra for the synthetic giniite samples that contained Al and SO_4 substitutions exhibited slight shifts in the position of some peaks relative to the pure end-member (e.g., Giniite-12 in Figure 13). The giniite from

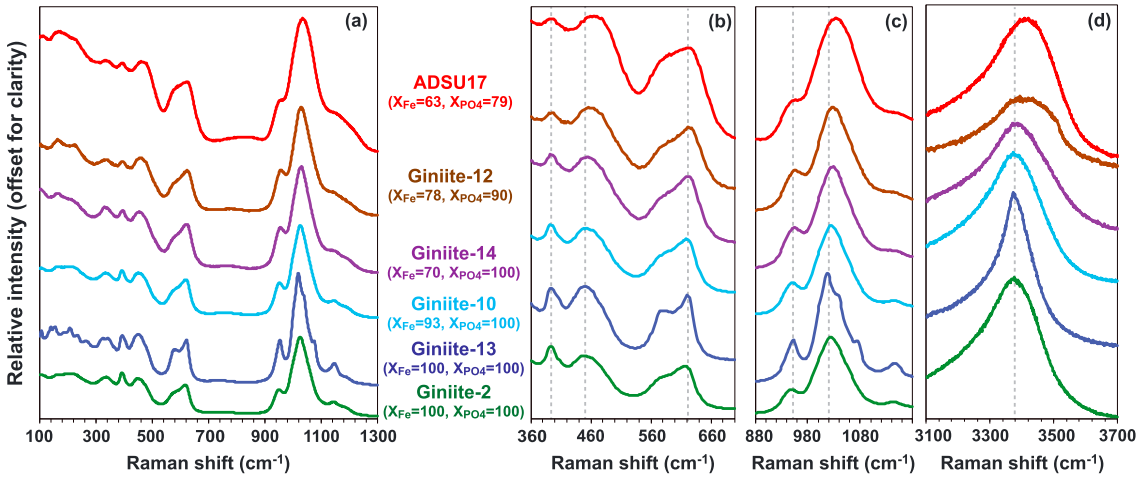

Figure 13. Representative Raman spectrum of the Fe-phosphate mineral present in reacted ADSU17 cinders compared with spectra for several synthetic giniite samples of varying chemical composition. Spectra are offset on the vertical scale for clarity. Note the slightly higher Raman shift values for some peaks in samples containing Fe-for-Al and SO_4-for-PO_4 substitutions as indicated by the X_{Fe} and X_{PO4} numbers (X_{Fe} = 100 × Fe/(Fe + Al) and X_{PO4} = 100 × P/(P + S), both on molar basis). Sample Giniite-13 was synthesized at a slightly higher temperature than the other samples (200 °C versus 185 °C), which resulted in sharper Raman features. See Frost et al. (2007) for a detailed discussion of the Raman spectra of giniite.

the experiment most closely matches the spectra for synthetic samples containing these substitutions, consistent with compositions measured by EDS. Crystal shapes of the synthetic giniites ranged from four-pointed stars to spheroids, with various intermediate forms (Figure S6). However, none of the synthetic samples exhibited the elongated tetragonal crystal morphology observed in the experiments (Figure 12b). Hausrath et al. (2013) similarly observed precipitation of giniite during experimental acid-sulfate alteration of mixtures of olivine, basaltic glass, and apatite at 150 °C. In their experiments, however, the giniite took on a spheroidal morphology rather than the elongated shape observed in our alteration experiments. Hausrath et al. (2013) also noted the presence of Al in their giniite precipitates.

A MB spectrum obtained for synthetic giniite was fit with a pair of doublets attributed to Fe^{III} (Figure 14), with fitting parameters listed in Table 1. The fitting parameters are similar to those derived for synthetic giniite by Hausrath et al. (2013), although those authors fit the spectrum with a single doublet (Table 1). On the other hand, Rouzies et al. (1994) fit the MB spectrum for their synthetic giniite with four doublets, with two doublets attributed to Fe^{II} and two to Fe^{III} (Table 1). However, Rouzies et al. (1994) synthesized their giniite from an Fe^{II}-bearing precursor, while the giniite produced for the present study (as well as in Hausrath et al., 2013) was synthesized using an Fe^{III}-bearing precursor (see the supporting information). As a consequence, the giniite synthesized for this study is likely composed entirely of Fe^{III}, whereas some Fe^{II} was present in the samples analyzed by Rouzies et al. (1994).

Analysis of the reacted basalt from experiment ADSU17 using MB spectroscopy resulted in identification of four doublets (Table 1 and Figure 14). Three of the doublets corresponded to Fe-bearing natroalunite and relict igneous phases (olivine and augite/glass). The remaining doublet is likely attributable to Fe^{III} in giniite, although the derived MB parameters (quadrapole splitting and isomer shift) for the doublet in the ADSU17 sample differ somewhat from those measured for the synthetic giniite. It is possible that the MB parameters for the giniite in ADSU17 are shifted slightly owing to the presence of Al and SO_4 substitutions in the mineral structure.

7. Discussion

7.1. Phosphorous Sequestration in the Burns Formation Bedrocks

The geochemical data indicate that P has most likely experienced very little or no mobilization throughout the formation of the layered sulfate-rich bedrocks that constitute the Burns formation. The only viable alternative explanation for the close similarity of the P abundances and P_2O_5:TiO_2 ratios of the Burns formation bedrocks to those of numerous examples of relatively unaltered Martian basalts would be that P was

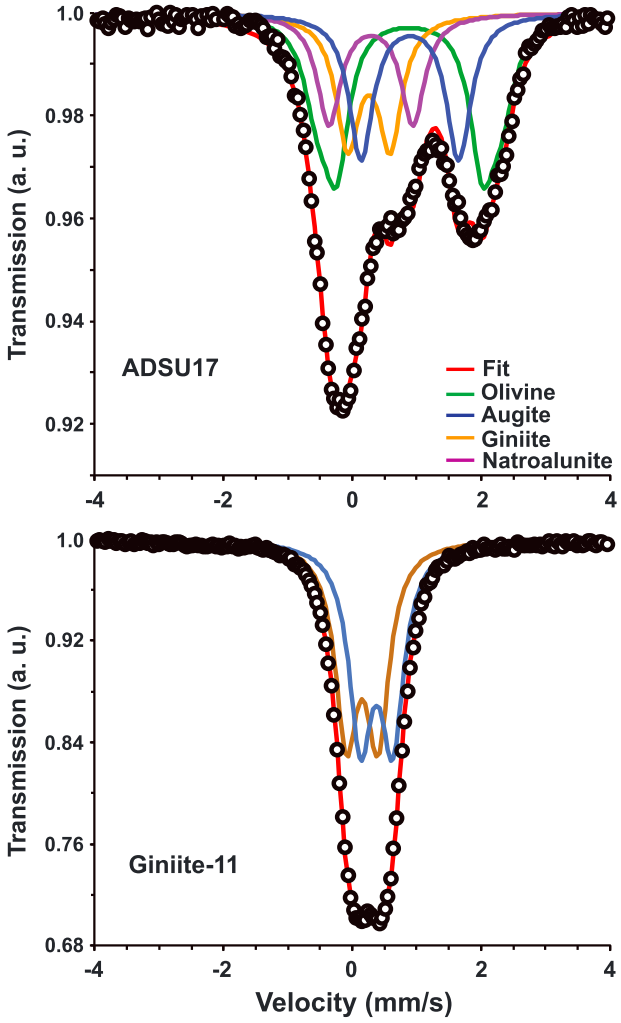

Figure 14. Mossbauer spectra for (a) experimentally altered basalt cinders (ADSU-17) and (b) synthetic giniite (Giniite-11). The circles are measured values, while the red lines are total fits to the data based on the doublets shown in each panels.

transported out of the precursor basaltic material at an early stage in the formation of the deposits, and then replaced in nearly identical amounts at a later stage. This, however, would require a rather remarkable coincidence between the amounts of P transported out of and then back into the materials, and is therefore an unlikely explanation for the observed compositions.

In unaltered crystalline basalts on the surface of Mars, most of the P is likely contained within Ca-phosphate minerals such as apatite and merrillite (Adcock & Hausrath, 2015; McSween & Treiman, 1998; McSween et al., 2008). Since primary Ca-phosphate minerals have higher solubilities under acidic conditions, it seems unlikely that the P could have persisted as Ca-phosphates in the Burns bedrocks. Instead, the P is probably sequestered in some less soluble form, either as a component from the original basalt other than Ca-phosphate or as a secondary phase with substantially lower solubility than the primary phosphate minerals.

Observations from field and laboratory studies suggest several potential reservoirs for P in the Burns formation bedrocks. One possibility is that the P is present within a relatively unreactive glass phase, either dissolved in the glass itself or as microcrystals of phosphate minerals protected within the glass. Although basaltic glass is generally thought to dissolve rapidly under acidic conditions (e.g., Brantley, 2008; Gislason & Oelkers, 2003), investigation of acid-sulfate alteration of basalt cinders at CN indicated that the glass is relatively unreactive and persists long after phenocrysts of plagioclase, augite, and olivine have been almost completely altered (McCollom, Hynek, et al., 2013; McCollom, Robbins, et al., 2013). Similar observations have been also reported for other acid-sulfate environments (e.g., Africano & Bernard, 2000). If analogous circumstances prevailed during alteration of the basaltic materials that were the precursor to the silicate component of the Burns formation, a relatively unaltered glass phase (and any microcrystals protected within it) might still persist in the deposits. Deconvolution of thermal emission spectra indicates that glass could constitute as much as 25% of the light-toned outcrops at Meridiani (Glotch et al., 2006), although this should be considered as a maximum value since the spectral component would also include amorphous silica, which is likely to be present in some amount. However, mass balance constraints would require the glass phase (or protected microcrystals) to contain a very high concentration

Table 1
Mössbauer Parameters for Altered Basalt Cinders From Experiment ADSU17 and for Synthetic Giniites

Sample	QS (mm/s)	IS (mm/s)	%	Assignment
ADSU17	0.37	0.39	13	Fe^{III} (giniite?)
	1.10	0.41	25	Fe^{III} (natroalunite)
	1.86	0.98	44	Fe^{II} (augite/glass)
	2.67	1.03	18	Fe^{II} (olivine)
Giniite-11	0.49	0.28	49	Fe^{III}
	0.49	0.50	51	Fe^{III}
Synthetic giniite (Rouzies et al., 1994)	1.05	0.42	42	Fe^{III}
	0.41	0.44	24	Fe^{III}
	2.61	1.15	11	Fe^{II}
	2.12	1.24	11	Fe^{II}
Synthetic giniite (Hausrath et al., 2013)	0.54	0.40	100	Fe^{III}

Note. QS = quadrupole splitting and IS = isomer shift.

of P (>4 wt% P_2O_5) in order to account for the bulk abundances measured in the bedrocks, and it is not clear that this is reasonable.

Another possibility is that the P is sequestered in less soluble phosphate minerals such as Fe- or Al-phosphates. In the laboratory experiments with CN basalt, apatite rapidly decomposed and the phosphate reprecipitated as the Fe-phosphate mineral giniite. Similar processes may have occurred during initial alteration of the basaltic component of the Burns formation. Precipitation of giniite was also observed by Hausrath et al. (2013) during experimental acid-sulfate alteration of mixtures of olivine, basaltic glass, and apatite at 150 °C, and unidentified Fe-phosphates were found among the products of lower temperature (25 °C) acid-sulfate alteration of synthetic Martian basalts with P_2O_5 concentrations comparable to those of the Meridiani deposits (Tosca et al., 2004). Collectively, these results suggest that Fe-phosphates are good candidates to sequester P in altered basaltic rocks on Mars and may limit its mobility. Aluminum phosphate minerals such as berlinite and variscite are also possible candidates.

Based on thermodynamic calculations, Berger et al. (2016) argued that PO_4 dissolved from primary phosphates in Martian basalts should reprecipitate as Fe-phosphate minerals from acidic fluids at high ionic strengths. Furthermore, those authors suggested that this process could explain the persistence of relatively high P abundances in rocks from the Murray formation in Gale crater that have been leached of several other elements by acidic fluids (e.g., Yen et al., 2017). The geochemical models of Berger et al. (2016) are based on solubility of the mineral strengite since this is the only Fe-phosphate mineral for which thermodynamic data are currently available in standard databases, but it is likely that other Fe-phosphates would also be stable under similar conditions. Given the prominent role of acidic, high-salinity fluids in the precipitation of the sulfate minerals of the Burns formation, a similar process might help to explain the immobility of P during formation of the rocks at Meridiani.

The studies where precipitation of giniite or other Fe-phosphates have been observed during experimental alteration of basalt were performed under closed-system conditions with relatively low fluid:rock ratios (Hausrath et al., 2013; Tosca et al., 2004; this study). Consequently, it remains uncertain whether such minerals would persist under more open-system conditions like those that may have prevailed during the development of the Burns formation. Persistence of minerals such as Fe- and Al-phosphates under open-system conditions depends on a number of factors, including the solubility of the minerals, their thermodynamic stability relative to other P-bearing phases, the compositions of infiltrating fluids, fluid:rock ratios, and the duration of fluid–rock interactions. Exploration of these issues by future experimental and modeling studies (e.g., Berger et al., 2016) will help to resolve the extent to which Fe- and Al-phosphates can sequester P in open-system environments like the Burns formation. Still, the experiments demonstrate that conversion of Ca-phosphates to Fe-phosphates during the early stages in the development of the Burns formation deposits is a plausible possibility.

Although giniite or other Fe-phosphates have not been identified with the MB spectrometer on Opportunity, it is not clear that they would be easily detectable owing to relatively low abundance and potential overlap of their MB signatures with sulfates and other phases (e.g., Dyar et al., 2014). For example, if all of the P_2O_5 measured in the Burns formation bedrocks were present as giniite, it would account for ~8% of the total amount of Fe in the rocks, compared with 24–35% for the component identified as jarosite and 16–26% assigned to the unidentified F3D3 component (Morris et al., 2006). Giniite has MB parameters (Table 1) that are similar to those of the Fe3D3 component (isomer shift ≈ 0.37, quadrapole splitting ≈ 0.65; Morris et al., 2006), and it would be difficult to discriminate giniite from this component. Curiosity or other future missions might be able to identify Fe-phosphates such as giniite using alternative methods such as XRD, Raman spectroscopy, or visible and near-infrared spectroscopy (e.g., Figure 13).

Another potential reservoir for P in the Burns formation could be jarosite or other members of the alunite mineral group. The most widely occurring members of the alunite group have molecular formulas that can be portrayed in general as $(K,Na,H_3O^+)(Al,Fe)_3(SO_4)_2(OH)_6$, where minerals with Fe≫ Al constitute the jarosite subgroup while those with Al≫ Fe constitute the alunite subgroup. Based on results of the MB spectrometer onboard the Opportunity rover, it has been proposed that minerals of the jarosite subgroup constitute a substantial fraction of the Burns formation bedrocks (Klingelhöfer et al., 2004; Morris et al., 2006). Although this phase has been widely referred to as jarosite (which strictly speaking only refers to the K- and Fe-rich end-member), Morris et al. (2006) inferred that this component contains $Na > K > H_3O^+$ and possibly

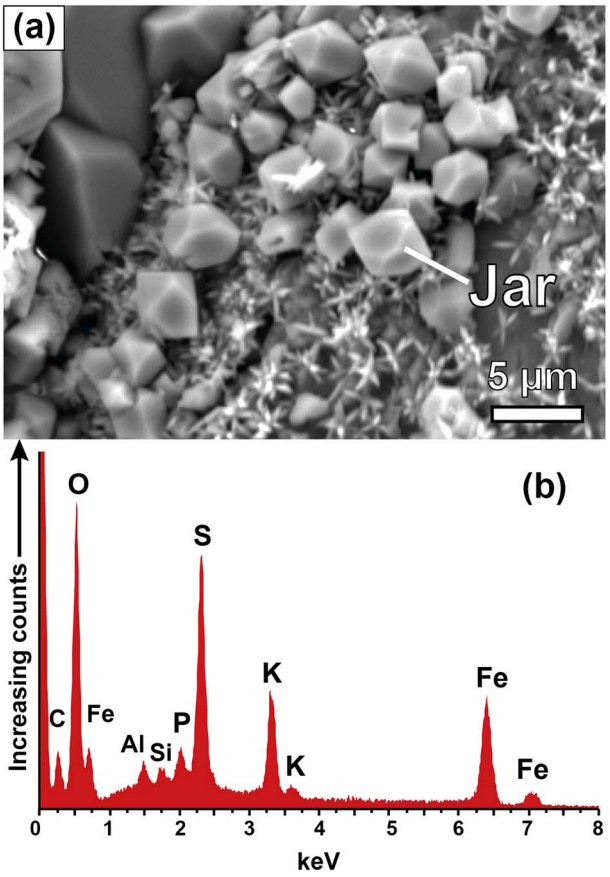

Figure 15. (a) Back-scattered electron image of jarosite crystals (Jar) in pore space of quartz-rich sandstone from the Aztec Formation, southeastern Nevada. (b) EDS spectrum from jarosite showing the presence of P and Al, indicative of PO_4-for-SO_4 and Al-for-Fe substitutions. Electron microprobe analysis of the sample indicates that in this sample, PO_4 replaces about ~10 mol% of the SO_4 in the jarosite structure.

some Al-for-Fe substitution (which would technically make it an Al-bearing natrojarosite). It is worth noting, however, that the MB signal that has been attributed to jarosite is also very similar to that of Fe-bearing natroalunite (McCollom, Hynek, et al., 2013, 2014), so an even broader range of mineral compositions within the alunite group could be consistent with the MB measurements.

Substitution of PO_4 for SO_4 can occur in jarosite and other members of the alunite group, allowing these minerals to be a significant reservoir for P (e.g., Dill, 2001; Scott, 1987). An example is provided in Figure 15, which shows jarosite crystals precipitated within a quartz-rich sandstone from the Aztec Formation in southwestern Nevada. Chemical analysis of the jarosite indicates that ~10% of the SO_4 site is occupied by PO_4, and even higher PO_4 contents are possible in members of this mineral group (Scott, 1987). A similar level of replacement of PO_4 in the jarosite (or other alunite group minerals) from the Burns formation could account for most or all of the P observed in the samples. Other structurally related minerals within the broader alunite supergroup are also possible reservoirs of P at Meridiani, such as woodhouseite [$CaAl_3(PO_4)(SO_4)(OH)_6$].

Still another possibility is that the P is adsorbed onto the surfaces of other minerals. Laboratory experiments have demonstrated that substantial amount of PO_4^{3-} can be adsorbed onto the surfaces of minerals such as nanophase Al- and Fe-oxides/oxyhydroxides, hematite, or jarosite (Rampe et al., 2016; Zhao et al., 2014). However, it is not clear that there are sufficient amounts of these phases present with enough surface area to account for the relatively large amount of P present in the Burns formation deposits, or whether the adsorption would be sufficiently strong to keep the P immobile through multiple episodes of fluid-rock interactions. Furthermore, experimental results indicate that adsorption of SO_4^{2-} outcompetes that of PO_4^{3-} for available sites (Zhao et al., 2014), suggesting that adsorption of PO_4^{3-} in sulfate-rich solutions may be limited. For these reasons, adsorption seems to be a less likely reservoir for P in the Burns formation bedrocks than other possibilities.

7.2. Implications for Alternative Formation Scenarios

The limited mobility of P during formation of the layered sulfate bedrocks of the Burns formation provides additional constraints on the sequence of events leading up to their present chemical and mineralogical composition, as well as the environmental conditions present during those events. The various scenarios that have been proposed to explain the origin of the bedrocks make very different assumptions about the settings and processes involved in their formation (Berger et al., 2009; McCollom & Hynek, 2005; McLennan et al., 2005; Niles & Michalski, 2009; Squyres et al., 2004; Squyres, Knoll, et al., 2006; Tréguier et al., 2008). In order to be compatible with the geochemical data, it must be demonstrable that the processes invoked in each scenario could be consistent with the apparent immobility of P. While the development of detailed geochemical models to test the compatibility of the various proposed scenarios with the immobility of P is beyond the scope of the present study, it is possible to make some general inferences about the processes that might have been involved.

In the sedimentary-evaporite scenario, the Burns formation deposits are proposed to have formed under relatively open system conditions where multiple elements, including a large fraction of the divalent cations (Fe, Mg, and Ca) in addition to S, were first transported out of and then back into the materials at different stages (Hurowitz et al., 2006; McLennan et al., 2005; Squyres et al., 2004; Squyres, Knoll, et al., 2006; Tosca et al., 2005). Mobilization of these elements is proposed to have been facilitated by acidic sulfate-rich fluids. To be compatible with the apparent immobility of P, conditions would have had to allow these fluids to mobilize SO_4

together with the divalent cations (and possibly other elements as well) without transporting significant amounts of P.

The initial step in the proposed sedimentary-evaporite scenario involved chemical alteration of pristine basalt to remove ~55% of the divalent cations (Squyres, Knoll, et al., 2006). Although the process responsible for the transport of these cations out of the basalt has not been identified, it presumably involved reaction with acidic fluids, and also caused precipitation of secondary silicate phases. Since it seems unlikely that any primary Ca-phosphate minerals that were originally present in the basalt could have survived alteration that was sufficiently intense to remove a large fraction of the divalent cations, sequestration of P into some less soluble secondary phase during this stage would probably be required to explain why it was not mobilized at the same time.

Following the initial alteration of the precursor basalt and removal of divalent cations, it is proposed that acidic fluids transported divalent cations together with SO_4 into the altered basalts and then evaporated, resulting in precipitation of Fe-, Mg-, and Ca-sulfate minerals (Squyres, Knoll, et al., 2006; Tosca et al., 2005). Tosca et al. (2005) performed geochemical models to simulate this process and showed that evaporation of fluids derived from low-temperature reaction of simulated Martian basalts with sulfuric acid in laboratory experiments (Tosca et al., 2004) should result in precipitation of a suite of sulfate minerals that are apparently compatible with the sedimentary-evaporite scenario. The geochemical models did not specifically address the possibility of mobilization of P into the materials by the evaporating fluid, but fluids derived from low-temperature acid-sulfate alteration of basalt could presumably have a limited capacity to transport P if this element was sequestered into phases with low solubility during alteration. Indeed, Tosca et al. (2004) noted the presence of Fe-phosphate minerals in several of their experiments, as well as possible adsorption of P onto Fe-oxide minerals. Nevertheless, it is notable that the fluids in some of the more acidic basalt alteration experiments of Tosca et al. (2004) contained millimolar concentrations of PO_4, and such fluids would presumably have the capacity to transport significant amounts of P and deposit it in minerals during evaporation. Additional experimental and modeling studies that focus on fate of P during alteration and evaporation could help clarify the conditions under which divalent cations could have been mobilized into the altered basaltic precursor without simultaneously mobilizing P.

Other scenarios propose that the sulfate-cemented siliciclastic sediments that comprise the Burns formation originally formed by addition of an oxidized S component to pristine basalt from atmospheric or volcanic sources without the addition of other chemical elements (Berger et al., 2009; McCollom & Hynek, 2005; Niles & Michalski, 2009; Tréguier et al., 2008). These scenarios propose that SO_2 or SO_3 form the atmosphere or volcanic vapors reacted with H_2O to form sulfuric acid, which then infiltrated and reacted with basalt to form sulfate minerals and other secondary products. These scenarios would probably require alteration at a relatively low fluid:rock ratio in order to maintain compositions that are closely similar to those of Martian basalts. If this were not the case, excess fluids would likely have migrated out of the materials and removed some of the chemical elements from the original basalt along with them. At low fluid:rock ratios, reaction with the acidic fluid would have dissolved the solid components of the basalt, and nearly all of the elements released would reprecipitate locally as secondary phases. Under such conditions, the system can be open to inputs of S and O from atmospheric or volcanic sources, while being closed with respect to all other chemical elements.

Because S and O are proposed to be the only elements transported into the basaltic precursor in these scenarios, the materials would have inherited the abundances of all other elements from the original basalt. Accordingly, the abundances of P_2O_5 and TiO_2 (as well as the P_2O_5:TiO_2 ratios) in the Burns formation bedrocks are presumed to reflect the composition of the original basalt, although the absolute abundances of P_2O_5 and TiO_2 would be diluted somewhat from the original basaltic values by the addition of SO_4 (i.e., green arrow in Figure 7a). Since elemental immobility is a basic assumption of these scenarios, they are inherently consistent with the apparent immobility of P during the initial stages of formation of the sediments. Based on the average composition of the Burns formation bedrocks recalculated to remove added SO_3, the original basalt precursor would presumably have contained ~1.4 wt% P_2O_5 and ~1.0 wt% TiO_2, which is well within the range of abundances and P_2O_5:TiO_2 ratios measured for relatively unaltered Martian basalts (see Data Set S1 and Figure S3).

Laboratory experiments suggest that primary Ca-phosphates are likely to be replaced by Fe-phosphates during acid-sulfate alteration of basalt under closed-system conditions (Hausrath et al., 2013; Tosca et al., 2004;

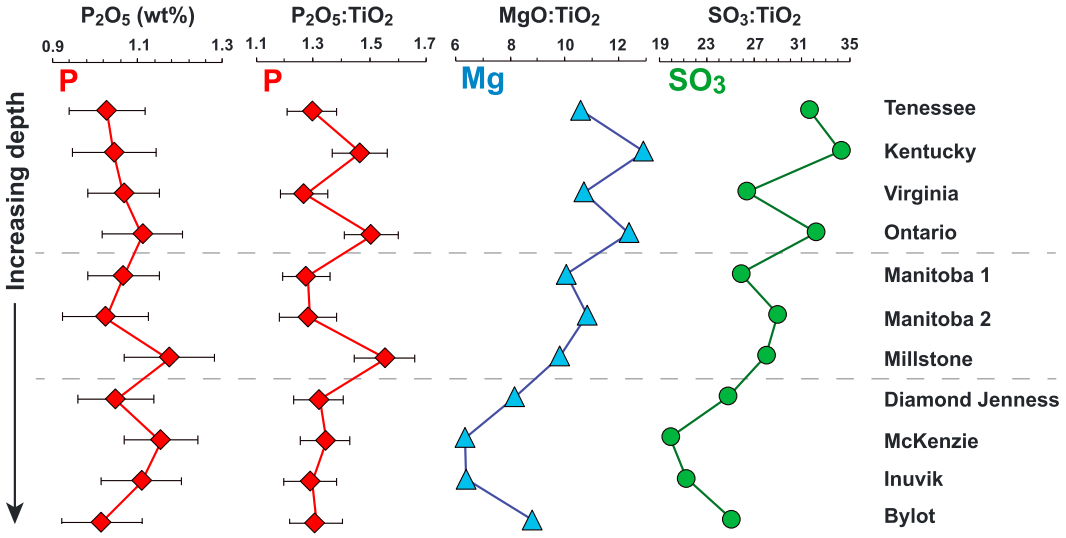

Figure 16. Variation in the abundance of P_2O_5 and oxide:TiO_2 ratios with depth in Burns formation bedrock within Endurance crater at Meridiani Planum (Figure 1). Estimated error bars are included for the P_2O_5 but are equal to or smaller than the size of the symbols for MgO and SO_3. The gray dashed lines indicate the positions of the Whatanga (upper) and Wellington (lower) contacts relative to the samples (Figure 1b). Note that the vertical scale shows relative depths and is not linear. A diagram showing the sample locations within the crater can be found in Clark et al. (2005).

this study). If this occurred during alteration of the basaltic precursor of the Burns formation deposits, Fe-phosphates may have been present along with sulfate minerals as components of the sand grains that were transported and deposited on Meridiani Planum. Unless P was transported into or out of the sand grains by subsequent processes, its abundance and P_2O_5:TiO_2 ratio would remain at that of the original basalt precursor.

After the sulfate-cemented silicate sands were transported from their original source location and deposited at Meridiani, they were apparently exposed to one or more episodes of groundwater infiltration that induced a number of diagenetic changes in the sediments, including precipitation of the hematite spherules that are characteristic of the site, dissolution of some phases leaving behind elongated crystal-shaped voids, and precipitation of secondary minerals that helped cement the deposits together (Grotzinger et al., 2005; McLennan et al., 2005). The presence of jarosite (or other members of the alunite-jarosite group) in the bedrocks would indicate that the fluids interacting with the deposits during diagenesis were at least moderately acidic and sulfate-rich (e.g., Elwood Madden et al., 2004; Klingelhöfer et al., 2004; Morris et al., 2006). In addition to other diagenetic changes, examination of the chemical compositions of bedrocks in a cross section of the Burns formation exposed in Endurance crater (Figure 1) showed a coupled decrease in the abundances of SO_3 and MgO with increasing depth in the formation (Clark et al., 2005). This trend suggests that infiltrating groundwaters may have partially dissolved some Mg-sulfate minerals and transported the components out of the deposits (Clark et al., 2005; Hurowitz & Fischer, 2014). Transport of MgO and SO_3 out of the deeper deposits is further supported by substantial decreases in the MgO:TiO_2 and SO_3:TiO_2 ratios in the lower parts of the section (Figure 16), reflecting loss of these components relative to the presumably immobile element Ti. Mass balance indicates that up to 40% of the MgO and SO_3 have been removed from samples in the deeper parts of the exposed section.

At the same time, the abundance of P_2O_5 and the P_2O_5:TiO_2 ratios remain essentially constant with depth (Figure 16), indicating that whatever process removed MgO and SO_3 from the lower deposits did not mobilize any of the P. Transport of MgO and SO_3 out of the deposits would require that the infiltrating fluid was initially undersaturated with respect to Mg-sulfate minerals so that dissolution of these minerals would occur. The absence of significant mobilization of P by these same fluids could potentially be explained by (a) the fluids already being saturated with respect to whatever P-bearing phase is present in the bedrocks so that dissolution did not occur, (b) P being sequestered in a phase with very low solubility under the conditions of the infiltrating fluid (pH, salinity, temperature, etc.) so that no detectable loss of this element occurred, or

(c) slow dissolution kinetics of the P-bearing phase on the timescales of the groundwater infiltration event. Application of reactive transport models that include P-bearing minerals (e.g., Adcock & Hausrath, 2015) to investigate chemical variation in the cross section of the Burns formation exposed in Endurance crater would help to test scenarios for removal of Mg-sulfate minerals and resolve which explanation is most likely to have been responsible for the apparent immobility of P during this event.

Other authors have noted a correlation between the high abundance of P with elevated concentrations of S and Cl in the Meridiani bedrocks and interpreted this to be an indication that PO_4 was transported into the deposits by aqueous fluids along with SO_4 and Cl (Greenwood & Blake, 2006; Rieder et al., 2004). In one study, these observations were used to argue for the existence of a global acidic aquifer or ocean on early Mars (Greenwood & Blake, 2006). However, the results of the present study indicate that it is highly unlikely that any significant amount of P was transported into the rocks by aqueous fluids. Instead, the high abundance of P is most likely a reflection of the composition of the basaltic precursor.

8. Concluding Remarks

The results of this study indicate that P can remain immobile, even under some acid-sulfate conditions where most other elements are mobilized during fluid-rock interaction. This result contrasts with other examples of Martian rocks and soils where mobilization of P by aqueous fluids has been invoked to explain observed enrichments or depletion of this element (e.g., Adcock & Hausrath, 2015; Hausrath et al., 2013; Hurowitz et al., 2006; Ming et al., 2006, 2008; Yen et al., 2008;). On the other hand, P also appears to have remained largely immobile while most other elements were leached out of the rock by acidic aqueous fluids during formation of alteration haloes around fractures in the Stimson and Murray formations in Gale crater (Yen et al., 2017). These contrasting results are likely an indication that several factors may combine to determine whether P is mobile or not, and the presence of acidic conditions alone is not sufficient to expect P to be mobilized.

The experimental results reported here and elsewhere (Hausrath et al., 2013; Tosca et al., 2004) as well as thermodynamic models (Berger et al., 2016) suggest that Fe-phosphates are one of the leading candidates for secondary minerals that may precipitate and limit P mobility during alteration of Martian basalts. Owing to potential overlap with other minerals, MB spectroscopy may not be particularly well suited to uniquely identify these minerals if they are present (e.g., Dyar et al., 2014). However, other techniques such as XRD, Raman spectroscopy, and visible and near-infrared spectroscopy may be useful in this respect for future missions. In addition to mineral identification, these analytical methods may offer the opportunity to place constraints on the chemical composition of phosphate minerals (e.g., Figure 13), potentially providing additional information about the chemical and physical environments in which they form.

Finally, reactive transport models have the potential to be a very useful tool to quantitatively test scenarios for the mobility of P in the Burns formation and other Martian deposits. These kinds of models have the capacity to simultaneously consider several factors that can affect mobility, including the solubility of minerals, the relative thermodynamic stability of different P-bearing phases, and fluid:rock ratio. However, development of such models is severely hampered at the present time by the lack of basic thermodynamic data for phosphate minerals, particularly Fe-phosphates. For example, strengite is the only Fe-phosphate mineral included in the most widely available thermodynamic databases for geochemical modeling, and data for this mineral are limited to 25 °C. As a consequence, construction of robust geochemical models of P mobility will probably need to be preceded by development of thermodynamic databases that include additional phosphate minerals.

Acknowledgments
This work was supported by funds from NASA Mars Fundamental Research Program grant NNX12AI02G and Mars Data Analysis Program grant NNX16AJ40G. The authors thank Bethany Ehlmann for providing spectral analysis of minerals and Karyn Rogers and Sally Potter-McIntyre for assistance with fieldwork. The authors are grateful for the comments of the reviewers and Editor that helped to refine our interpretations and improve the manuscript. All data discussed in this report are included in the spreadsheets provided as supporting information. The Institute for Rock Magnetism is supported by the Instruments and Facilities Program of the NSF Division of Earth Science. This is IRM contribution number 1709. The authors declare no financial conflicts of interest.

References

Adcock, C. T., & Hausrath, E. M. (2015). Weathering profiles in phosphorous-rich rocks at Gusev crater, Mars, suggest dissolution of phosphate minerals into potentially habitable near-neutral waters. *Astrobiology*, *15*(12), 1060–1075. https://doi.org/10.1089/ast.2015.1291

Adcock, C. T., Hausrath, E. M., & Foster, P. M. (2013). Readily available phosphate from minerals in early aqueous environments on Mars. *Nature Geoscience*, *6*(10), 824–827. https://doi.org/10.1038/ngeo1923

Africano, F., & Bernard, A. (2000). Acid alteration in the fumaroles environment of the Usu volcano, Hokkaido, Japan. *Journal of Volcanology and Geothermal Research*, *97*(1-4), 475–495. https://doi.org/10.1016/S0377-0273(99)00162-6

Agee, C. B., Wilson, N. V., McCubbin, F. M., Ziegler, K., Polyak, V. J., Sharp, Z. D., et al. (2013). Unique meteorite from Early Amazonian Mars: Water-rich basaltic breccia Northwest Africa 7034. *Science*, *339*(6121), 780–785. https://doi.org/10.1126/science.1228858

Arvidson, R. E., Ashley, J. W., Bell, J. F. III, Chojnacki, M., Cohen, J., Economou, T. E., et al. (2011). Opportunity Mars Rover mission: Overview and selected results from Purgatory ripple to traverses to Endeavour crater. *Journal of Geophysical Research*, *116*, E00F15. https://doi.org/10.1029/2010JE003746

Arvidson, R. E., Bell, J. F. III, Catalano, J. G., Clark, B. C., Fox, V. K., Gellert, R., et al. (2015). Mars Reconnaissance Orbiter and Opportunity observations of the Burns formation: Crater hopping at Meridiani Planum. *Journal of Geophysical Research: Planets*, *120*, 429–451. https://doi.org/10.1002/2014JE004686

Arvidson, R. E., Poulet, F., Morris, R. V., Bibring, J.-P., Bell, J. F. III, Squyres, S. W., et al. (2006). Nature and origin of the hematite-bearing plains of Terra Meridiani based on analyses of orbital and Mars Exploration Rover data sets. *Journal of Geophysical Research*, *111*, E12S08. https://doi.org/10.1029/2006JE002728

Baratoux, D., Samuel, H., Michaut, C., Toplis, M. J., Monnereau, M., Wieczorek, M., et al. (2014). Petrological constraints on the density of the Martian crust. *Journal of Geophysical Research: Planets*, *119*, 1707–1727. https://doi.org/10.1002/2014JE004642

Barrat, J. A., Jambon, A., Bohn, M., Gillet, P., Sautter, V., Göpel, C., et al. (2002). Petrology and chemistry of the Picritic Shergottite North West Africa 1068 (NWA 1068). *Geochimica et Cosmochimica Acta*, *66*(19), 3505–3518. https://doi.org/10.1016/S0016-7037(02)00934-1

Berger, G., Toplis, M. J., Tréguier, E., D'Uston, C., & Pinet, P. (2009). Evidence in favor of small amounts of ephemeral and transient water during alteration at Meridiani Planum, Mars. *American Mineralogist*, *94*(8-9), 1279–1282. https://doi.org/10.2138/am.2009.3230

Berger, J. A., Schmidt, M. E., Izawa, M. R. M., Gellert, R., Ming, D. W., Rampe, E. B., et al. (2016). Phosphate stability in diagenetic fluids constrains the acidic alteration model for lower Mt. Sharp sedimentary rocks in Gale crater, *Mars*. Paper presented at Lunar & Planetary Science Conference XLVII, Lunar and Planetary Institute, Houston, TX.

Brantley, S. L. (2008). Kinetics of mineral dissolution. In S. L. Brantley & J. D. Kubicki (Eds.), *Kinetics of Water-Rock Interactions* (pp. 151–210). New York: Springer.

Clark, B. C., Morris, R. V., McLennan, S. M., Gellert, R., Jolliff, B., Squyres, S. W., et al. (2005). Chemistry and mineralogy of outcrops at Meridiani Planum. *Earth and Planetary Science Letters*, *240*(1), 73–94. https://doi.org/10.1016/j.epsl.2005.09.040

Cornu, S., Lucas, Y., Lebon, E., Ambrosi, J. P., Luizão, F., Rouillet, J., et al. (1999). Evidence of titanium mobility in soil profiles, Manaus, central Amazonia. *Geoderma*, *91*(3-4), 281–295. https://doi.org/10.1016/S0016-7061(99)00007-5

Crossley, R. J., Evans, K. A., Reddy, S. M., & Lester, G. W. (2017). Redistribution of iron and titanium in high-pressure ultramafic rocks. *Geochemistry, Geophysics, Geosystems*, *18*, 3869–3890. https://doi.org/10.1002/2017GC007145

Crovisier, J. L., Honnorez, J., & Eberhart, J. P. (1987). Dissolution of basaltic glass in seawater: Mechanism and rate. *Geochimica et Cosmochimica Acta*, *51*(11), 2977–2990. https://doi.org/10.1016/0016-7037(87)90371-1

Dill, H. G. (2001). The geology of aluminium phosphates and sulphates of the alunite group minerals: A review. *Earth-Science Reviews*, *53*(1-2), 35–93. https://doi.org/10.1016/S0012-8252(00)00035-0

Dyar, M. D., Jawin, E. R., Breves, E., Marchand, G., Nelms, M., Lane, M. D., et al. (2014). Mössbauer parameters of iron in phosphate minerals: Implications for interpretation of Martian data. *American Mineralogist*, *99*(5-6), 914–942. https://doi.org/10.2138/am.2014.4701

Elwood Madden, M. E., Bodnar, R. J., & Rimstidt, J. D. (2004). Jarosite as an indicator of water-limited chemical weathering on Mars. *Nature*, *431*(7010), 821–823. https://doi.org/10.1038/nature02971

Frost, R. L., Wills, R., & Martens, W. N. (2007). A Raman spectroscopic study of synthetic giniite. *Spectrochimica Acta*, *66*(1), 42–47. https://doi.org/10.1016/j.saa.2006.02.018

Galvez, M. E., Beyssac, O., Benzerara, K., Menguy, N., Bernard, S., & Cox, S. C. (2012). Micro- and nano-textural evidence of Ti(-Ca-Fe) mobility during fluid-rock interactions in carbonaceous lawsonite-bearing rocks from New Zealand. *Contributions to Mineralogy and Petrology*, *164*(5), 895–914. https://doi.org/10.1007/s00410-012-0780-2

Gellert, R., Rieder, R., Brückner, J., Clark, B. C., Dreibus, G., Klingelhöfer, G., et al. (2006). Alpha Particle X-Ray Spectrometer (APXS): Results from Gusev crater and calibration report. *Journal of Geophysical Research*, *111*, E02S05. https://doi.org/10.1029/2005JE002555

Gislason, S. R., & Oelkers, E. H. (2003). Mechanisms, rates, and consequences of basaltic glass dissolution: II. An experimental study of the dissolution rates of basaltic glass as a function of pH and temperature. *Geochimica et Cosmochimica Acta*, *67*(20), 3817–3832. https://doi.org/10.1016/S0016-7037(03)00176-5

Glotch, T. D., & Bandfield, J. L. (2006). Determination and interpretation of surface and atmospheric Miniature Thermal Emission Spectrometer spectral end-members at the Meridiani Planum landing site. *Journal of Geophysical Research*, *111*, E12S06. https://doi.org/10.1029/2005JE002671

Glotch, T. D., Bandfield, J. L., Christensen, P. R., Calvin, W. M., McLennan, S. M., Clark, B. C., et al. (2006). Mineralogy of the light-toned outcrop at Meridiani Planum as seen by the Miniature Thermal Emission Spectrometer and implications for their formation. *Journal of Geophysical Research*, *111*, E12S03. https://doi.org/10.1029/2005JE002672

Greenwood, J. P., & Blake, R. E. (2006). Evidence for an acidic ocean on Mars from phosphorus geochemistry of Martian soils and rocks. *Geology*, *34*(11), 953–956. https://doi.org/10.1130/G22415A.1

Grotzinger, J. P., Arvidson, R. E., Bell, J. F. III, Calvin, W., Clark, B. C., Fike, D. A., et al. (2005). Stratigraphy and sedimentology of a dry to wet eolian depositional system, Burns formation, Meridiani Planum, Mars. *Earth and Planetary Science Letters*, *240*(1), 11–72. https://doi.org/10.1016/j.epsl.2005.09.039

Guidry, M. W., & Mackenzie, F. T. (2003). Experimental study of igneous and sedimentary apatite dissolution: Control of pH, distance from equilibrium, and temperature on dissolution rates. *Geochimica et Cosmochimica Acta*, *67*(16), 2949–2963. https://doi.org/10.1016/S0016-7037(03)00265-5

Harouiya, N., Chaïrat, C., Köhler, S. J., Gout, R., & Oelkers, E. H. (2007). The dissolution kinetics and apparent solubility of natural apatite in closed reactors at temperatures from 5 to 50 °C and pH from 1 to 6. *Chemical Geology*, *244*(3-4), 554–568. https://doi.org/10.1016/j.chemgeo.2007.07.011

Hausrath, E. M., Golden, D. C., Morris, R. V., Agresti, D. G., & Ming, D. W. (2013). Acid sulfate alteration of fluorapatite, basaltic glass and olivine by hydrothermal vapors and fluids: Implications for fumarolic activity and and secondary phosphate phases in sulfate-rich Paso Robles soil at Gusev crater, Mars. *Journal of Geophysical Research: Planets*, *118*, 1–13. https://doi.org/10.1029/2012JE004246

Hausrath, E. M., Navarre-Sitchler, A. K., Sak, P. B., Steefel, C. I., & Brantley, S. L. (2008). Basalt weathering rates on Earth and the duration of liquid water on the plains of Gusev crater, Mars. *Geology*, *36*(1), 67–70. https://doi.org/10.1130/G24238A.1

Hurowitz, J. A., & Fischer, W. W. (2014). Contrasting styles of water-rock interaction at the Mars Exploration Rover landing sites. *Geochimica et Cosmochimica Acta*, *127*, 25–38. https://doi.org/10.1016/j.gca.2013.11.021

Hurowitz, J. A., McLennan, S. M., McSween, H. Y. Jr., DeSouza, P. A. Jr., & Klingelhöfer, G. (2006). In situ and experimental evidence for acidic weathering of rocks and soils on Mars. *Journal of Geophysical Research*, *111*, E02S19. https://doi.org/10.1029/2005JE002515

Hynek, B. M., McCollom, T. M., Marcucci, E., Brugman, K., & Rogers, K. (2013). Assessment of environmental controls on acid-sulfate alteration at active volcanoes in Nicaragua: Applications to relic hydrothermal systems on Mars. *Journal of Geophysical Research: Planets*, *118*, 2083–2104. https://doi.org/10.1002/jgre.20140

Klingelhöfer, G., Morris, R. V., Bernhardt, B., Schröder, C., Rodionov, D. S., de Souza, P. A. Jr., et al. (2004). Jarosite and hematite at Meridiani Planum from Opportunity's Mössbauer spectrometer. *Science*, *306*(5702), 1740–1745. https://doi.org/10.1126/science.1104653

Lane, M. D., Bishop, J. L., Dyar, M. D., King, P. L., Parente, M., & Hyde, B. C. (2008). Mineralogy of the Paso Robles soils on Mars. *American Mineralogist*, *93*(5-6), 728–739. https://doi.org/10.2138/am.2008.2757

Lodders, K. (1998). A survey of shergottite, nakhlite and chassigny meteorites whole-rock compositions. *Meteoritics and Planetary Science*, *33*(S4), A183–A190. https://doi.org/10.1111/j.1945-5100.1998.tb01331.x

Longhi, J., Knittle, E., Holloway, J. R., & Wänke, H. (1992). The bulk composition, mineralogy and internal structure of Mars. In H. H. Kieffer, et al. (Eds.), *Mars* (pp. 184–208). Tucson, AZ: University of Arizona Press.

Markússon, S. H., & Stefánsson, A. (2011). Geothermal surface alteration of basalts, Krýsuvík Iceland—Alteration mineralogy, water chemistry and the effects of acid supply on the alteration process. *Journal of Volcanic and Geothermal Research*, *206*(1-2), 46–59. https://doi.org/10.1016/j.jvolgeores.2011.05.007

McCollom, T. M., Ehlmann, B. L., Wang, A., Hynek, B. M., Rogers, K., Moskowitz, B., & Berquó, T. S. (2014). Detection of iron substitution in natroalunite-natrojarosite solid solutions and potential implications for Mars. *American Mineralogist*, *99*(5-6), 948–964. https://doi.org/10.2138/am.2014.4617

McCollom, T. M., & Hynek, B. M. (2005). A volcanic environment for bedrock diagenesis at Meridiani Planum, Mars. *Nature*, *438*(7071), 1129–1131. https://doi.org/10.1038/nature04390

McCollom, T. M., Hynek, B. M., Rogers, K., Moskowitz, B., & Berquó, T. S. (2013). Chemical and mineralogical trends during acid-sulfate alteration of pyroclastic basalt at Cerro Negro volcano, and implications for early Mars. *Journal of Geophysical Research: Planets*, *118*, 1719–1751. https://doi.org/10.1002/jgre.20114

McCollom, T. M., Robbins, M., Moskowitz, B., Berquó, T. S., Jöns, N., & Hynek, B. M. (2013). Experimental study of acid-sulfate alteration of basalt and implications for sulfate deposits on Mars. *Journal of Geophysical Research: Planets*, *118*, 577–614. https://doi.org/10.1002/jgre.20044

McHenry, L. J. (2009). Element mobility during zeolitic and argillic alteration of volcanic ash in a closed-system lacustrine environment: Case study Olduvai Gorge, Tanzania. *Chemical Geology*, *265*(3-4), 540–552. https://doi.org/10.1016/j.chemgeo.2009.05.019

McLennan, S. M., Bell, J. F. III, Calvin, W. M., Christensen, P. R., Clark, B. C., de Souza, P. A. Jr., et al. (2005). Provenance and diageneis of the evaporate-bearing Burns formation, Meridiani Planum, Mars. *Earth and Planetary Science Letters*, *240*(1), 95–121. https://doi.org/10.1016/j.epsl.2005.09.041

McSween, H., & Treiman, A. H. (1998). Martian meteorites. In J. Papike (Ed.), *Planetary Materials*, *Reviews in Mineralogy and Geochemistry* (Vol. 36, pp. F1–F53). Washington, DC: Mineral Society of America.

McSween, H. Y., Ruff, S. W., Morris, R. V., Gellert, R., Klingelhöfer, G., Christensen, P. R., et al. (2008). Mineralogy of volcanic rocks in Gusev crater, Mars: Reconciling Mössbauer, Alpha particle X-Ray Spectrometer, and Miniature Thermal Emission Spectrometer spectra. *Journal of Geophysical Research*, *113*, E06S04. https://doi.org/10.1029/2007JE002970

Ming, D. W., Gellert, R., Morris, R. V., Arvidson, R. E., Brückner, J., Clark, B. C., et al. (2008). Geochemical properties of rocks and soils in Gusev crater, Mars: Results of the Alpha Particle X-Ray Spectrometer from Cumberland Ridge to Home Plate. *Journal of Geophysical Research*, *113*, E12S39. https://doi.org/10.1029/2008JE003195

Ming, D. W., Mittlefehldt, D. W., Morris, R. V., Golden, D. C., Gellert, R., Clark, B. C., et al. (2006). Geochemical and mineralogical indicators for aqueous processes in the Columbia Hills of Gusev crater, Mars. *Journal of Geophysical Research*, *111*, E02S12. https://doi.org/10.1029/2005JE002560

Morris, R. V., Klingelhöfer, G., Schröder, C., Rodionov, D. S., Yen, A., Ming, D. W., et al. (2006). Mossbauer mineralogy of rock, soil, and dust at Meridiani Planum, Mars: Opportunity's journey across sulfate-rich outcrop, basaltic sand and dust, and hematite lag deposits. *Journal of Geophysical Research*, *111*, E12S15. https://doi.org/10.1029/2006JE002791

Niles, P. B., & Michalski, J. (2009). Meridiani Planum sediments on Mars formed though weathering in massive ice deposits. *Nature Geoscience*, *2*(3), 215–220. https://doi.org/10.1038/ngeo438

Papike, J. J., Keith, T. E. C., Spilde, M. N., Galbreath, K. C., Shearer, C. K., & Laul, J. C. (1991). Geochemisty and mineralogy of fumarolic deposits, Valley of Ten Thousand Smokes, Alaska: Bulk chemical and mineralogical evolution of dacite-rich protolith. *American Mineralogist*, *76*, 1662–1673.

Rampe, E. B., Morris, R. V., Archer, D. P. Jr., Agresti, D. G., & Ming, D. W. (2016). Recognizing sulfate and phosphate complexes chemisorbed onto nanophase weathering products on Mars using in-situ and remote observations. *American Mineralogist*, *101*(3), 678–689. https://doi.org/10.2138/am-2016-5408CCBYNCND

Rieder, R., Gellert, R., Anderson, R. C., Brückner, J., Clark, B. C., Dreibus, G., et al. (2004). Chemistry of rocks and soils at Meridiani Planum from the Alpha Particle X-ray Spectrometer. *Science*, *306*(5702), 1746–1749. https://doi.org/10.1126/science.1104358

Rouzies, D., Varlous, J., & Millet, J. M. M. (1994). Thermal behavious and physic-chemical characterization of synthetic and natural iron hydroxyphosphates. *Journal of the Chemical Society, Faraday Transactions*, *92*, 3335–3339.

Ruff, S. W., Niles, P. B., Alfano, F., & Clarke, A. B. (2014). Evidence for a Noachian-aged ephemeral lake in Gusev crater, Mars. *Geology*, *42*(4), 359–362. https://doi.org/10.1130/G35508.1

Scott, K. M. (1987). Solid solution in, and classification of, gassan-derived members of the alunite-jarosite family, northwest Queensland, Australia. *American Mineralogist*, *72*, 178–187.

Squyres, S. W., Arvidson, R. E., Blaney, D. L., Clark, B. C., Crumpler, L., et al. (2006). Rocks of the Columbia Hills. *Journal of Geophysical Research*, *111*, E02S11. https://doi.org/10.1029/2005JE002562

Squyres, S. W., Grotzinger, J. P., Arvidson, R. E., Bell, J. F. III, Calvin, W., Christensen, P. R., et al. (2004). In situ evidence for an ancient aqueous environment at Meridiani Planum, Mars. *Science*, *306*(5702), 1709–1714. https://doi.org/10.1126/science.1104559

Squyres, S. W., Knoll, A. H., Arvidson, R. E., Clark, B. C., Grotzinger, J. P., Jolliff, B. L., et al. (2006). Two years at Meridiani Planum: Results from the opportunity rover. *Science*, *313*(5792), 1403–1407. https://doi.org/10.1126/science.1130890

Sun, S.-s., & McDonough, W. F. (1989). Chemical and isotopic systematics of oceanic basalts: Implications for mantle composition and processes. In A. D. Saunders & M. J. Norry (Eds.), *Magmatism in the Ocean Basins*, *Geological Society Special Publication* (Vol. 36, pp. 313–345). Oxford: Geological Society.

Tosca, N. J., McLennan, S. M., Clark, B. C., Grotzinger, J. P., Hurowitz, J. A., Knoll, A. H., et al. (2005). Geochemical modeling of evaporation processes on Mars: Insight from the sedimentary record at Meridiani Planum. *Earth and Planetary Science Letters*, *240*(1), 122–148. https://doi.org/10.1016/j.epsl.2005.09.042

Tosca, N. J., McLennan, S. M., Lindsley, D. H., & Schoonen, M. A. A. (2004). Acid-sulfate weathering of synthetic Martian basalt: The acid fog model revisited. *Journal of Geophysical Research*, *109*, E05003. https://doi.org/10.1029/2003JE002218

Tréguier, E., d'Uston, C., Pinet, P. C., Berger, G., Toplis, M. J., McCoy, T. J., et al. (2008). Overview of Mars surface geochemical diversity through Alpha Particle X-Ray Spectrometer data multidimensional analysis: First attempt at modeling rock alteration. *Journal of Geophysical Research*, *113*, E12S34. https://doi.org/10.1029/2007JE003010

Treiman, A. H., & Filiberto, J. (2015). Geochemical diversity of shergottite baslats: Mixing and fractionation, and their relation to Mars surface basalts. *Meteoritics & Planetary Science*, *50*(4), 632–648. https://doi.org/10.1111/maps.12363

Usui, T., McSween, H. Y. Jr., & Clark, C. C. III (2008). Petrogenesis of high-phosphorous Wishstone Class rocks in Guseve Crater, Mars. *Journal of Geophysical Research*, *113*, E12S44. https://doi.org/10.1029/2008JE003225

Van Baalen, M. R. (1993). Titanium mobility in metamorphic systems: A review. *Chemical Geology*, *110*(1-3), 233–249. https://doi.org/10.1016/0009-2541(93)90256-I

Wänke, H., Brückner, J., Dreibus, G., Rieder, R., & Ryabchikov, I. (2001). Chemical composition of rocks and soils at the Pathfinder site. *Space Science Reviews*, *96*(1/4), 317–330. https://doi.org/10.1023/A:1011961725645

Yen, A. S., Ming, D. W., Vaniman, D. T., Gellert, R., Blake, D. F., Morris, R. V., et al. (2017). Multiple stages of aqueous alteration along fractures in mudstone and sandstone strata in Gale crater, Mars. *Earth and Planetary Science Letters*, *471*, 186–198. https://doi.org/10.1016/j.epsl.2017.04.033

Yen, A. S., Morris, R. V., Clark, B. C., Gellert, R., Knudson, A. T., Squyres, S., et al. (2008). Hydrothermal processes at Gusev crater: An evaluation of Paso Robles class soils. *Journal of Geophysical Research*, *113*, E06S10. https://doi.org/10.1029/2007JE002978

Zhao, Y.-Y. S., McLennan, S. J., & Schoonen, M. A. (2014). Behavior of bromide, chloride, and phosphate during low-temperature aqueous Fe(II) oxidation processes on Mars. *Journal of Geophysical Research: Planets*, *119*, 998–1012. https://doi.org/10.1002/2013JE004417

Zolotov, M. Y., & Shock, E. L. (2005). Formation of jarostie-bearing deposits through aqueous oxidation of pyrite at Meridiani Planum, Mars. *Geophysical Research Letters*, *32*, L21203. https://doi.org/10.1029/2005GL024253

Zolotov, M. Y., & Mironenko, M. V. (2016). Chemical models or Martian weathering profiles: Insights into formation of layered phyllosilicate and sulfate deposits. *Icarus*, *275*, 203–220. https://doi.org/10.1016/j.icarus.2016.04.011